The establishment and characterization of an improved cell-free assay for exocytosis in neuroendocrine PC12 cells

PhD Thesis

in partial fulfilment of the requirements
for the degree “Doctor of Philosophy (PhD)”
in the Neuroscience Program
at the Georg August University Göttingen,
Faculty of Biology

submitted by

Marcin Barszczewski

born in

Warsaw, Poland

2005

Declaration

This thesis has been written independently and with no other sources and aids than required.

Marcin Barszczewski

15th May 2005

Contents

Abbreviations

AMP-PNP	–	adenosine 5′-(β,γ-imido) triphosphate
ATP	–	adenosine 5'-triphosphate
ATPγS	–	adenosine-5'-O- (3-thiotriphosphate)
BoNT	–	botulinum neurotoxin
BSA	–	bovine serum albumin
CCD	–	charge-coupled device
Cy3 / 5	–	derivatives of cyanin fluorescent dyes
ddH_2O	–	double-distilled water
DMEM	–	Dulbecco's modified Eagle medium
DMSO	–	dimethyl sulfoxide
DPTA	–	1,3-diamino-2-propanol-N,N,N',N'-tetraacetic acid
DTT	–	dithiothreitol
EDTA	–	ethylenediamine-tetraacetic acid
EGTA	–	ethyleneglycol-*bis*(β-aminoethyl)-N,N,N′,N′-tetraacetic acid
FCS	–	foetal calf serum
GTP	–	guanosine 5'-triphosphate
HEPES	–	N-[2-hydroxyethyl]-piperazine-N'-[2-ethanesulphonic acid]
hNPY-eGFP	–	human neuropeptide Y fused to enhanced green fluorescent protein
IPTG	–	isopropyl-ß-D-thiogalactopyranoside

K-Glu	–	potassium glutamate
LDCV	–	large dense core vesicle
NEM	–	N-ethylmaleimide
Ni-NTA	–	Ni^{2+}-nitrilotriacetic acid
NSF	–	NEM sensitive fusion protein
PBS	–	phosphate-buffered saline
PC12	–	cells of rat pheochromocytoma tumor
PFA	–	paraformaldehyde
PIPES	–	piperazine-N,N'-bis(2-ethanesulfonic acid)
PMSF	–	phenyl methyl sulfonyl fluoride
RBC	–	rat brain cytosol
ROI	–	region of interest
RRP	–	readily releasable pool
RT	–	room temperature
SDS	–	sodium dodecyl sulphate
SDS-PAGE	–	SDS-polyacrylamide gel electrophoresis
SNAP	–	soluble NSF attachment protein
SNAP-23	–	synaptosome-associated protein 23 kilo Dalton
SNAP-25	–	synaptosome-associated protein 25 kilo Dalton
SN25	–	SNAP-25
SNARE	–	SNAP receptors
SRP	–	slowly releasable pool
Syb 2	–	synaptobrevin 2

Syx 1	–	syntaxin 1
TE	–	Tris/EDTA buffer
TeNT	–	tetanus neurotoxin
TIRFM	–	total internal reflection fluorescence microscopy
TMA-DPH	–	1-(4-trimethylammonium)-6-phenyl-1,3,5-hexatriene
Tris	–	2-amino-2-(hydroxymethyl)-1,3-propanediol
UPP	–	unprimed pool
VAMP2	–	vesicle-associated membrane protein 2 = synaptobrevin 2
w/v	–	weight-to-volume ratio

1. Introduction

Neurotransmitter- or hormone–loaded secretory granules fuse with the plasma membrane in a regulated manner and this process of exocytosis is precisely controlled by a vast array of mechanisms. Exocytosis involves many precisely orchestrated steps that occur prior to fusion which include (1) dislocation of a secretory vesicle from cytoplasm to cortical regions of the plasma membrane, (2) vesicle attachment to the plasma membrane, referred to as tethering/docking, to membrane-associated macromolecular complexes with subsequent (3) vesicle priming and (4) Ca^{2+}-triggered fusion.

Over the past years, results of physiological and biochemical experiments provided insights into each of the above-outlined discrete steps preceding the fusion of a secretory granule with the plasma membrane, however the exact nature and order of biochemical reactions in which they occur remains to be elucidated. In particular, not much is known about the molecular mechanisms of docking and priming.

In the next chapters, it will be discussed what are the proposed mechanisms and the hypothesized key players that regulate the late stages of secretory organelle exocytosis.

1.1. The pre-fusion stages of the exocytotic pathway

In contrast to the advanced understanding of the membrane fusion reaction itself, less is known about the steps prior to the formation of molecular complexes that drive it.

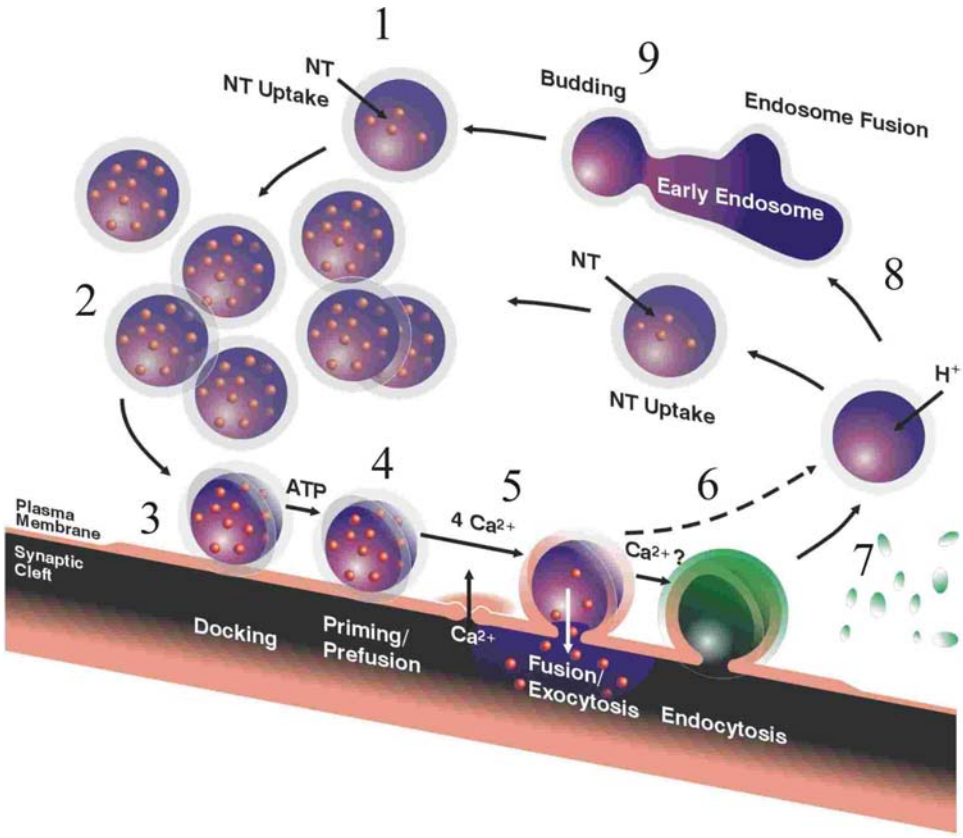

Figure 1 **– The synaptic vesicle cycle**

The synaptic vesicles are loaded with neurotransmitter (1) and form a reserve (or depot) pool (2). From the reserve pool they are translocated to the proximity of plasma membrane (3), where the vesicles most likely undergo activation through many obscure processes collectively referred to as priming (4). Only the fully primed vesicles would respond rapidly to the inbound Ca^{2+} and thus fuse with the plasma membrane releasing their content – the neurotransmitter molecules (5). After partial or full release of neurotransmitter

the vesicles need to be retrieved through different modes of endocytosis. These may involve reusing of the vesicle soon after exocytotic discharge (6), retrieval of vesicle with involvement of clathrin (7) or re-arrangements occurring via various endosomal routes (8,9). Figure was reproduced and modified with permission of Dr M.G. Holt.

1.1.1. Biogenesis of secretory organelles

Secretory granules originate in the *trans*-Golgi network and have to undergo series of maturation steps before entering regulated secretory pathway (Tooze et al., 2001). These steps include protein sorting, enzymatic processing and membrane compaction which all lead to the formation of a mature, large dense-core vesicle (LDCVs). Once such organelles are fully assembled, they are transported to the close proximity of the plasma membrane.

1.1.2. Translocation, tethering and docking of secretory vesicles

1.1.2.1. Translocation

Mobilization of vesicles from the cytoplasm and their placement in the cortical region of the cell precedes the reactions of tethering and docking (Pfeffer, 1999). It has been postulated that ATP-Mg is required for mobilization of vesicles by ATP-Mg-dependent motors such as myosin II and its Ca^{2+}-regulated myosin light chain kinase. They are suspected to play a role during vesicle translocation to the cell membrane (Becker and Hart, 1999; Kumakura et al., 1994).

1.1.2.2. Tethering

It is believed that the tethering and docking are influenced by proteins belonging to the family of Ras-related Rab/ypt small GPTases (or Rabs) that undergo precisely regulated cycles of re- and dephosphorylation (Geppert et al., 1997; Novick and Zerial, 1997; Sogaard et al., 1994). This feature, combined with a high specificity of Rabs for their effectors suggests, that in the active, GTP-bound form, Rab proteins may shuttle back and forth sets of proteins recruiting them to sites of fusion. Such recruitment would lead to the creation of a specific biochemical tag located on the donor organelle. This in turn, would initiate outlining of protein supercomplexes taking active part in attaching two membranes together, a prerequisite for following priming reactions and subsequent fusion (Jahn et al., 2003; Zerial and McBride, 2001). It seems that SNARE proteins, the postulated catalysts of membrane fusion, are not directly involved in tight vesicle docking as their genetic or enzymatic ablation, e.g. in *Drosophila* abolishes fusion but does not stop docking (Broadie et al., 1995).

1.1.2.3. Docking

Docking takes place on a specialized part of neuronal membrane known as the active zone. These structures do not seem to be present in neuroendocrine cells (Thureson-Klein, 1983). The active zone proteins belong to several families, influencing various steps of fusion processes. Compartmentalisation of proteins and lipids in the active

zone indicates presence of a highly organized environment in which fusion occurs (Gundelfinger et al., 2003; Rohrbough and Broadie, 2005; Ziv and Garner, 2004).

Exocytosis has been intensively studied in neuroendocrine cells because like neurones, these cells undergo Ca^{2+}-triggered exocytosis and feature similar molecular machinery responsible for controlling and driving exocytosis. In addition, larger size of the neuroendocrine cells compared to a synaptic terminal makes measurements of exocytosis easier than in synapses of neurones. Also the effects of fusion of large, dense-core vesicles are more feasible for monitoring with e.g. patch-clamp amperometry in comparison to studies done on small synaptic vesicles operating in synaptic terminals.

In the neuroendocrine PC12 cell line, a large proportion of or LDCVs was shown to be morphologically docked, i.e. they were within 10 nm range from plasma membrane (Banerjee et al., 1996). Data obtained with total internal reflection fluorescence microscopy (TIRFM) have shown that mobile secretory granules approach the membrane, at which point their mobility decreases dramatically as they gradually become membrane-attached and immobile (Steyer et al., 1997). In some instances, previously docked secretory granules were observed to detach and withdraw into the cytoplasm. This raised a possibility that several docking stages may exist in neuroendocrine cells. During and after docking, the secretory granules start to undergo reactions of maturation and acquisition of fusion-competent status. These processes are referred to as priming.

1.1.3. Priming

Currently applied experimental assays for exocytosis take advantage of electrophysiological or biochemical techniques and often define priming in different ways. Priming processes involve several proteins and include multiple ATP-Mg-dependent and ATP-Mg-independent events along the secretory cascade (Chamberlain et al., 1995; Hay and Martin, 1993). Generally, priming can be characterized as a stepwise increase of associations between membranes that is essential for efficient, Ca^{2+}-triggered exocytosis proceeding after influx of Ca^{2+} ions. The processes of priming occur after tethering and docking and ultimately lead to attainment of fusion-competent state by docked secretory organelles (Parsons et al., 1995; Sorensen, 2004).

Importance of the energy supply for the maintenance of priming reactions has been underlined by the results from neuroendocrine cells perfused with non-hydrolysable analogues of ATP – ATPγS or AMP-PNP what caused a loss of the faster component of exocytosis (Xu et al., 1999; Xu et al., 1998). While no ATP-Mg appears to be needed in the final fusion reaction exocytosis (Hay and Martin, 1992; Heidelberger, 1998), it is not known at which stage ATP-Mg becomes expendable and what ATP-Mg-dependent reactions are required for the secretory organelles to reach a fusion competent state after docking.

1.1.3.1. Involvement of ATP in priming reactions

Based on the data gathered in several studies, it can be assumed that ATP-Mg is involved in at least three, likely concomitant, branches of reactions that contribute to the processes of priming.

Firstly, the ATP-Mg-dependent reactions include formation of phosphatidylinositol-4,5-phosphate-2 (PIP_2) by respective kinases (PI_4K and PIP_5K). Results of studies done in the Martin laboratory (Hay and Martin, 1993) showed that these proteins were required for the ATP-Mg-dependent priming of exocytosis (Wenk and De Camilli, 2004). Secondly, protein kinases: A (Koga and Takahashi, 2004) and C (Nagy et al., 2002; Perin et al., 1990), as well as phospholipase A_2 (Bloch-Shilderman et al., 2002) have both been implicated in regulatory protein phosphorylation increasing the Ca^{2+}-dependent release from PC12 cells. Finally, ATP-Mg is essential for the disassembly of biochemically stable *"cis"*-SNARE complexes. This process requires specialized machinery that provides means for the liberation of SNARE proteins.

Studies on proteins involved in the processes of disassembly, NSF and α-SNAP, were a large part of this thesis, therefore these factors will be discussed below in more detail.

1.1.3.2. Role of NSF and α-SNAP in priming

ATP-dependent SNARE complex disassembly is driven by AAA ATPase NSF and its co-factor α-SNAP (Patel and Latterich, 1998). A-SNAP is known to bind to the *"cis"*-SNARE complexes and in turn to recruit and activate NSF what liberates SNAREs from the complex. A-SNAP and its two homologues β- and γ-SNAP were originally discovered as factors required for recruiting NSF to membranes in cell-free transport assays (Clary and Rothman, 1990; Whiteheart et al., 2001). NSF and α-SNAP have been both shown to actively participate in all intracellular processes involving membrane fusion. It has been demonstrated that the functional NSF is indispensable for an uninterrupted cycling of SNARE proteins. The SNARE disassembly process is essential for the maintenance of synaptic function as shown in the *comatose* mutant of *Drosophila* (Littleton et al., 1998).

There are two models of α-SNAP function in the exocytotic pathway. The first one proposes that α-SNAP and NSF act after fusion to disassemble the resultant *"cis"*-SNARE complexes and to liberate the SNAREs that drove merger of membranes (Jahn et al., 2003; Sollner, 2003). In the other model, however, it is assumed that α-SNAP / NSF-dependent priming occurs prior to the fusion step and is needed to free the SNAREs from inactive *"cis"*-complex state to activate them for incoming fusion. This possibility assumes that SNAREs entangled into *"cis"*-complexes would reside in the membrane, where they would stay in an inactive state. The activation of

SNAREs could then occur only before fusion to prevent an illegitimate merger of organelles bearing cognate SNAREs (Banerjee et al., 1996).

1.2. The SNARE proteins

Among the factors involved in exocytosis, the soluble NSF receptor (SNARE) proteins are the best characterized as catalysts of the membrane fusion reaction (Sollner et al., 1993). They are involved in all the membrane fusion events in the secretory pathways in eukaryotic cells. The SNARE proteins belong to a large superfamily consisting of more than 60 members in yeast and mammalian cells (Bock et al., 2001). SNAREs are small, abundant and mostly membrane-bound proteins that share a common so-called SNARE motif allowing them for reversible assembly into tight, four-helix bundles – *"trans"*-SNARE complexes (Sutton et al., 1998). The readily formed metastable *"trans"* complexes are composed of three SNAREs: syntaxin 1 (Bennett et al., 1992) and SNAP-25 (Oyler et al., 1989) resident in cell membrane and synaptobrevin 2 (also referred to as vesicle-associated membrane protein or VAMP) anchored in the vesicular membrane (Trimble et al., 1988). Syntaxin and synaptobrevin are anchored in respective membranes by their C-terminal domains, whereas SNAP-25 is tethered to the plasma membrane via several cysteine-linked palmitoyl chains.

The plasma membrane-resident SNAREs have been shown to be present in distinct microdomains or clusters, the integrity of which is essential for the exocytotic competence of the cell (Chamberlain et al., 2001; Lang et al., 2001).

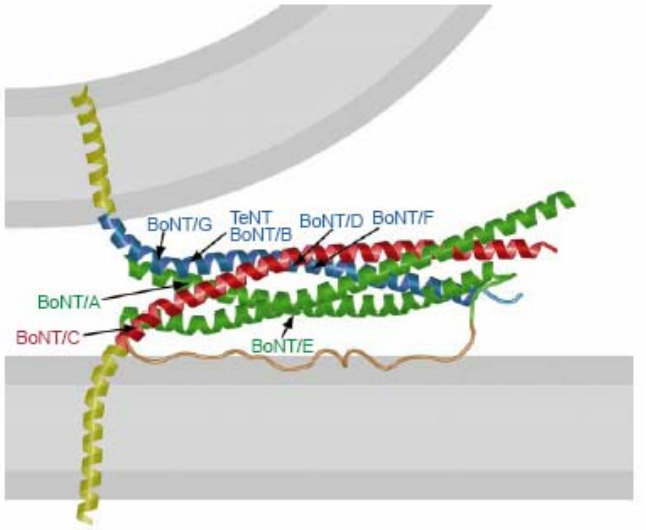

***Figure 2* – A model of SNARE-mediated bridging between the membranes of synaptic vesicle and presynaptic terminal**

The four α-helices of the synaptic SNARE proteins contribute to the formation of a ternary SNARE complex. The helix of vesicle-anchored synaptobrevin 2 is shown in blue, whereas the helices of presynaptic-resident Q-SNAREs – two of SNAP-25 and one of syntaxin 1 are labelled in green and red, respectively. Arrows indicate cleavage sites recognized by botulinum and tetanus neurotoxins – SNARE-specific peptidases from the family of clostridial toxins (modified after Sutton et al., 1998).

According to the "zipper" hypothesis (Sutton et al., 1998), the complex assembly starts at the N-terminal parts of SNARE motifs and proceeds towards the C-termini

that anchor interacting proteins in membranes. Formation of the *"trans"*-SNARE complex proceeds through an intermediate complex composed of SNAP-25 and syntaxin 1, which later accommodates synaptobrevin 2 (Fasshauer and Margittai, 2004). Assembly of the SNAREs into the *"trans"* complexes likely bridges the apposed lipid bilayers of membranes belonging to cell and secretory granule, bringing them in a close proximity and thereby inducing their fusion (Jahn and Hanson, 1998; Weber et al., 1998). It is believed that the influx of Ca^{2+} triggers the completion of the assembly reaction. This process is mediated by an interaction between the putative Ca^{2+}-sensor, synaptotagmin, with membrane lipids and/or the partially assembled SNARE complex (Brose et al., 1992; Fernandez-Chacon et al., 2001).

Based on the stability of the resultant "*cis*"-SNARE complex, it has been postulated that energy released during the assembly process serves as a means for overcoming the repulsive forces between the membranes (Lin and Scheller, 1997). There are several models that propose explanation of a subsequent step – the formation of stalk and fusion pore, but the exact nature of these processes remains debated (Jahn and Grubmuller, 2002). To date, it has not been ultimately clarified whether the SNAREs are responsible solely for bringing membranes to apposition or whether they are the driving force for fusion.

1.2.1. The cycle of SNARE proteins

A scheme presenting the cycle of SNARE proteins and postulated sites for α-SNAP and NSF action during exocytosis is shown in the next figure. The question of the site of α-SNAP/NSF action in the exocytotic pathway has been addressed in this thesis and is discussed in the later chapters.

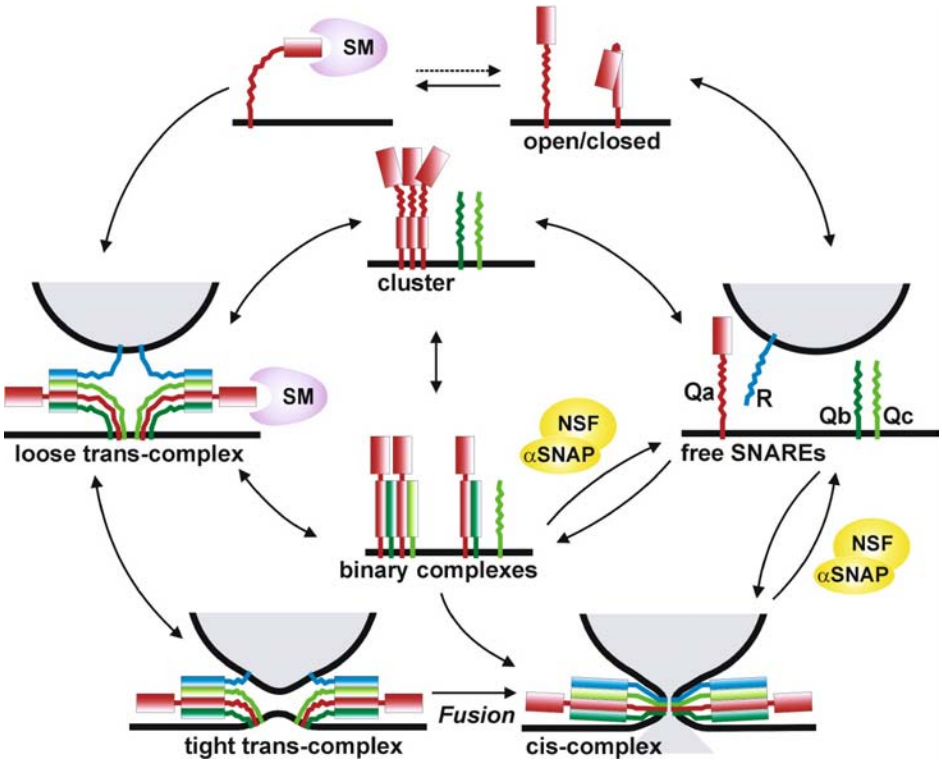

***Figure 3* – The cycle of SNARE proteins**

The free SNAREs contain unstructured SNARE motifs which undergo multiple interactions. It is believed, that the assembly of four SNARE motifs is a key reaction that allows for subsequent fusion of opposing membranes. Formation of the *"trans"*-complexes is thought to be reversible. Before fusion, *"trans"*-SNARE complexes may exist in interchangeable loose and tight

states. To reactivate SNAREs, i.e. allow them for entry into another round of fusion, the *"cis"*-SNARE complex requires ATP-Mg-dependent disassembly. This process is thought to involve NSF and its co-factor α-SNAP. It has been also proposed that α-SNAP and NSF prevent free SNAREs from spontaneous assembly and formation of inactive *"cis"*-SNARE complexes. Figure reproduced from (Jahn et al., 2003)

The exocytotic paradigm discussed earlier is present in neurones and neuroendocrine cells where both the Qa- and Qb-SNARE motifs are donated by one SNAP-25 molecule. In other intracellular trafficking routes these two motifs are located on various molecules contributing to the formation of non-neuronal SNARE complexes.

1.2.2. Interaction of SNAREs with modulators of their function

The processes of priming and fusion are influenced by many proteins binding directly to SNAREs. In particular, proteins of the Sec/Munc (SM) family have been shown to be especially important for the integrity of exocytotic pathway (Toonen and Verhage, 2003). One member of the SM family, Munc 18 (Hata *et al.,* 1993; Garcia *et al.,* 1994; Pevsner *et al.,* 1994) has been shown to bind to the N-terminal region in syntaxin 1. It is a matter of debate what is the role of Munc 18-syntaxin 1 interaction, as initially it is been claimed that Munc 18 stabilizes the "closed" conformation of syntaxin 1 (Dulubova *et al.,* 1999). Interestingly, the Munc 18 *null* phenotype shows virtually no neurotransmitter release and a very dramatic reduction in the number of membrane-docked LDCVs (Voets et al., 2001). Additionally, the Munc 18 interaction

with syntaxin 1 is impeded by other binding partners of syntaxin 1 – SNAP-25 and synaptobrevin 2. Furthermore, studies in a model nematode *Caenorhabditis elegans* demonstrated presence of a process of displacement of Munc 18 by a priming factor Munc 13 (Betz et al., 1996; Brose et al., 2000) bound to the N-terminal region in syntaxin 1 and this reaction has been postulated to additionally regulate Munc 18 availability. The important role of Munc 13 in priming has been demonstrated in Drosophila where genetic ablation of this protein stops the synaptic transmission and leads to the accumulation of secretory vesicles at the plasma membrane (Aravamundan et al., 1999)

1.2.2.1. Putative calcium sensors

Other proteins suspected of direct or indirect involvement in exocytosis are the putative calcium sensors synaptotagmins 1 and 2 (Brose et al., 1992; Geppert et al., 1991; Perin et al., 1990) and complexins (Ishizuka et al., 1995). Synaptotagmins interact with the SNARE complex and phospholipids that are crucial for Ca^{2+}-sensing (Fernandez-Chacon et al., 2001). Complexins have been shown to bind to the SNARE complexes (McMahon et al., 1995) and although not essential for secretion, they are thought to promote Ca^{2+}-sensing function of synaptotagmin 1 by stabilisation of the SNARE complex.

1.3. The vesicle pools model

Unraveling of the molecular steps leading towards membrane fusion has been supported by kinetic analyses of rapid responses recorded electrophysiologically in chromaffin cells.

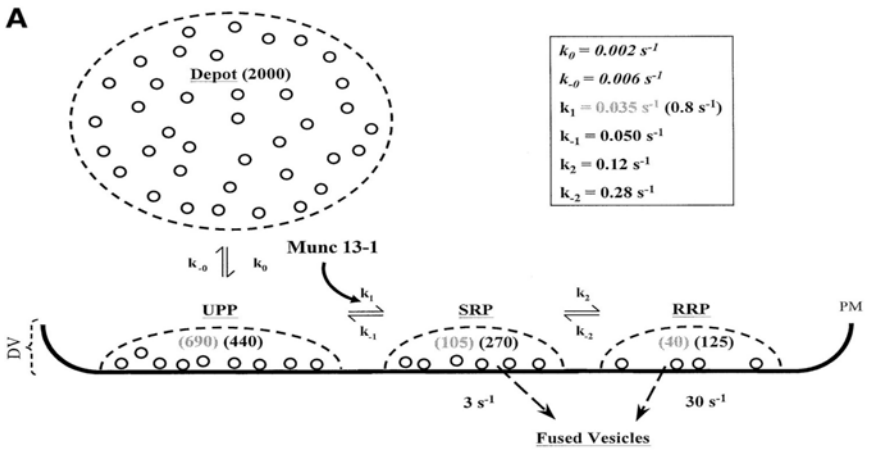

***Figure 4* – The model of sequential pools of vesicles in chromaffin cells**

In this model, different vesicle pools are in dynamic equilibrium before triggering of exocytosis. The size of the readily and slowly releasable pools (RRP, SRP) is reflected in the amplitude of the fast and slow burst exocytotic component Exponential time constants determine rates of fusion (dashed arrows). The sustained component reflects the priming rate and/or the size of the unprimed pool (UPP). Figure was modified after (Ashery et al., 2000).

Studies of LDCVs exocytosis in chromaffin cells postulated presence of at least three pools of vesicles in these cells. Firstly, the readily releasable pool (RRP) of the fully fusion-competent organelles contains vesicles that are ready in all respects to immediately react to influx of calcium ions and thereby to undergo Ca^{2+}-triggered

exocytosis. The second population is the slowly releasable pool (SRP) which encompasses vesicles that did not fully undergo priming processes, but which can replenish the RRP, and thus fuse briefly after completion of priming. Ultimately, the unprimed pool (UPP) contains docked granules that did not attain competence for fusion and need to go through several priming steps in order to become competent for exocytosis (Rettig and Neher, 2002).

This model proposed mapping of distinct kinetics components to various populations (or pools) of granules that would differ in readiness for fusion (Ashery et al., 2000). The measured time constants of transmitter release would hint at which stage on the exocytotic pathway a given pool of vesicles was. The above model suggests presence of several intermediate stages of readiness which may or may not reflect actual status of SNARE complex assembly.

1.4. Assays for exocytosis

Most of the knowledge concerning the molecular mechanisms of SNARE assembly, disassembly and SNARE-interacting proteins is based on studies of proteins in solution (Fasshauer et al., 1997). These studies do not however, allow for addressing questions concerning function of SNARE proteins in native and intact biological membranes. A different approach takes advantage of recombinant SNAREs reconstituted into proteoliposomes (Schuette et al., 2004; Weber et al., 1998). This allows for studying the minimal and essential molecular mechanisms required for driving fusion in artificial lipid membranes. To address physiological aspects of

exocytosis, the exocytotic processes outlined above had to be investigated with assays that bore resemblance to largely intact cells. This prompted the introduction of experimental systems based on permeabilized neuroendocrine cells (Holz et al., 1989) or assays derived from such cells (Ann et al., 1997; Hay and Martin, 1993; Linial and Parnas, 1996; Martin, 1989). These approaches allowed for only a limited range of biochemical studies due to a still high degree of complexity of the remaining underlying molecular reactions. Cells permeabilized by electrical or mechanical rupture, by detergent treatment or by pore-forming toxins, were instrumental in differentiating between the stages of exocytosis and identification of several factors required for these steps.

In most cell-free assays, exocytosis was studied with various biochemical tools perturbing the system and allowing for dissection of the exocytotic stages. Series of studies performed on purified synaptic preparations (Blasi et al., 1993a; Blasi et al., 1993b; Link et al., 1992; Niemann et al., 1994) revealed a fact that the SNARE proteins are the targets of specific clostridial neurotoxins what offered a chance to selectively knock-down SNAREs of interest. The SNARE proteins are highly susceptible to toxin attack in monomeric form, whereas they are protected to various degrees when entangled into *"trans"*- or *"cis"*-SNARE complexes (Chen et al., 1999; Montecucco et al., 1988; Schiavo et al., 2000). Toxin studies (Gerona et al., 2000) supported the notion of the presence of partially toxin-resistant complexes and pools of vesicles at different stages of complex assembly. They differed in readiness to Ca^{2+}-trigger initiating fusion of membranes. Complementary studies of exocytosis

in permeabilized neuroendocrine cells were performed with recombinant domains of SNAREs. They demonstrated that the SNARE complexes in PC12 cell can be inhibited differently before and complex assembly by application of these proteins fragments (Chen et al., 1999; Chen et al., 2001).

1.5. Limitation of previously used *in vitro* assays for exocytosis in PC12 cells

An assay providing a tool for studying exocytotic steps has been developed in the laboratory of Reinhard Jahn. It was a cell-free system for regulated exocytosis in the PC12 neuroendocrine cell line. Intact cells were incubated with acridine orange to load secretory granules. Ultrasonic shearing of PC12 cells grown on glass coverslips resulted in the generation of flat, inside-out membrane lawns that remained attached to the coverslip and that still contained docked secretory granules on them. Rise in Ca^{2+} levels triggered the exocytotic fusion of these objects with the plasma membrane. Monitoring of exocytosis was based on observation of acridine orange dequenching flashes (Avery et al., 2000). However, acridine orange-loaded secretory granules could not easily be imaged due to the severe photodamage of the dye preventing longer time-lapse acquisitions. Therefore an improved version of this assay has been established. Secretory granules were labelled with a hormonal content marker (hNPY) coupled to a variant of green fluorescent protein (eGFP), overcoming photodamage problem caused by the use of acridine orange (Holroyd et al., 2002; Lang et al., 2001).

However, one of the major limitations of these assays was the time-delay between the loss of cell integrity and the measurement of exocytosis, resulting in the biochemical run-down and loss of activated states. Reduction of this delay would allow for gaining direct access to the late steps in the exocytotic pathway, resembling the time window typically applied in whole-cell patch clamping experiments.

2. Methods

2.1. Cell culture

2.1.1. Propagation and seeding of cells

Rat pheochromocytoma (PC12, clone 251; Heumann et al. 1983) cells were grown in 75 cm^2 tissue culture flasks which contained 25 ml of growth medium - DMEM with high (4.5 g/l) glucose (Cambrex, New Jersey, USA). DMEM was supplemented with 10 % horse serum (Biochrom, Berlin), 5 % foetal calf serum "Gold", 4 mM L-glutamine, 60 U/ml penicillin, 60 µg/ml streptomycin (both from Cambrex) which all have been sterile filtered. For maintenance of a *Mycoplasma*-free cell culture, 6.25 µg/ml of Plasmocin (InvivoGen, San Diego, USA) was present in cell culture throughout entire period of its growth. Cells were grown at 37°C in 10 % CO_2 at 90 % relative humidity. For passaging, one flask of confluent cells (approximately 240000 cells/cm^2) was used. Growth medium was decanted followed by wash with 3 ml of trypsin/EDTA solution (Cambrex). Cells were detached from their substrate with 3 ml trypsin/EDTA. Trypsin activity on cells was blocked by addition of 27 ml of growth medium. Suspension of cells was centrifuged at 235 x g_{av} for 5 min at 20°C (Varifuge 3.0R, Heraeus-Kendro Sepatech, Langenselbold, Germany). Medium was removed and the resulting cell pellet was titurated in 10 ml of fresh growth medium. Cells were diluted at 1:2 – 1:4, transferred into 75 cm^2 un-coated tissue culture flasks (model 83.1813, Sarstedt, Nümbrecht, Germany) and passaged every 48-96 hrs depending on experimental needs. To avoid any undesired age-dependent

differentiation of culture, cells were used for only 20 passages since defrosting, after which new aliquot of liquid N_2-frozen cells would be used.

For seeding on glass coverslips, cells were detached from their substrate as described above, titurated and diluted to give a final concentration of approximately 600,000 cells/ml. 500 µl of this suspension (3 x 10^4 cells/cm^2) were evenly plated onto each poly-L-lysine-coated coverslip. After plating, cells were transferred to incubator and allowed to settle onto the coverslips for at least 30 min. 3 ml of growth medium were then added. Cells were used for experiments 48-72 hrs after plating.

2.1.2. Transient transfection of PC12 cells

Cells were passaged as above, but after trypsin treatment half of one flask's cells was titurated in cytomix buffer (after van den Hoff et al., 1992; 120 mM KCl, 10 mM KH_2PO_4, 10 mM K_2HPO_4, 0.15 mM $CaCl_2$, 2 mM EGTA, 5 mM $MgCl_2$, 2 mM ATP, 5 mM glutathione and 25 mM HEPES-KOH, pH 7.7, sterile filtered). ATP and glutathione were always added freshly to the cytomix shortly before re-suspension. 390 µl of cell suspension together with 80 µg of hNPY-eGFP plasmid DNA (Lang et al., 2001) were mixed in an electroporation cuvette (2 mm electrode gap, Biorad, Munich). An electric pulse was applied using a Biorad Genepulser II (settings: potential difference – 1.15 kV, resistance – 50 Ω, capacitance - 50 µF). Immediately after pulse application contents of the cuvette were then diluted with 2.6 ml of DMEM growth medium. 500 µl of the resulting suspension were plated onto poly-L-

lysine coated coverslips as described for un-transfected cells. Cells prepared in this manner were used for experiments 36 – 48 hrs after transfection.

2.1.3. Starting of a new cell culture

PC12 cells were stored as 1 ml aliquots in liquid nitrogen in FCS "Gold" containing 10 % DMSO (Sigma, Seelze, Germany). To start a culture, 1 ml aliquot of cells was rapidly defrosted and diluted into 10 ml of growth medium. Cells were spun down, resuspended in 10 ml of fresh growth medium, transferred into 25 cm^2 un-coated tissue culture flasks (model 3014, Falcon/BD, Bedford, MA, USA) and maintained as described above. To remove expelled traces of DMSO and dead cells debris, growth medium was always exchanged 24 hrs after splitting and then every 48 hrs. To eliminate possible *Mycoplasma* contamination from the freshly prepared cell culture 25 µg/ml of Plasmocin was added to cell culture during first five passages of dividing cells totalling approximately 3 weeks of treatment.

2.1.4. Coating of glass coverslips

For preparation of coated glass coverslips (Menzel Gläser, Braunschweig, Germany), they were thoroughly washed for 24 hrs in Decon 90 solution (Decon Laboratories, East Sussex, UK) and then cleansed ultrasonically in sonifier (Sonorex RK 100, Bandelin, Berlin) for 2 hrs in ultrapure water (Milli-Q®, Millipore) exchanged every 30 min. Ultimately, coverslips were rinsed in 100 % ethanol (Merck, Bad Soden, Germany) and briefly flamed. 500 µl of a 100 µg/ml poly-L-lysine hydrobromide

(molecular weight >300 kDa, Sigma, Cat. no: P-1524) solution was placed evenly onto each coverslip and incubated for 30 min at RT. This was followed by one wash with 1 ml sterile ultra pure H_2O. Coverslips were then air dried at RT for 90 min.

2.2. Recombinant proteins used in experiments

2.2.1. α-SNAP

The sequences for bovine α-SNAP and the mutant bovine α-SNAP (L294A) were each cloned into the pET28a vector (Novagen, San Diego, CA, USA) in frame with a sequence encoding for an N-terminally attached His_6-tag. For protein expression the constructs were transformed into *E. coli* BL21(DE) grown to a density of A_{600} = 1.0 in LB medium and induced for 3 h at 37°C with 0.25 mM isopropyl-thio-ß-D-galactoside (IPTG). After sonication the bacterial lysates were purified with a Ni^{2+}-nitrilotriacetic acid agarose (Ni-NTA) column eluting with 400mM imidazol. Following elution, His_6-tags were removed by thrombin cleavage during overnight dialysis. Further purification and concentration were achieved by an ion exchange chromatography step on the Äkta system (Amersham Biosciences, Freiburg, Germany) using a MonoQ column for wild-type α-SNAP as well as the α-SNAP (L294A) variant. A NaCl-gradient (0.1 – 1 M) was used for elution. All buffers involved in the purification were Tris-buffers (20 mM, pH 7.4) including 50 mM NaCl, 1 mM EDTA and 1 mM DTT. Finally the protein fractions were analysed by SDS-PAGE and their concentration was determined using the Bradford reagent (see below, BioRad).

2.2.2. NSF

Recombinant NSF was a kind gift of Ulrike Winter.

2.2.3. Light chains of clostridial neurotoxins

The following proteins: tetanus toxin (TeNT), botulinum toxins: A (BoNT A), C1, (BoNT C1), inactive C1 (BoNT C1 E230A) and E (BoNT E) were kind gifts of Alexander Stein, Felipe Zilly and Tabrez Siddiqui.

2.2.4. Synaptobrevin 2, SNAP-25, syntaxin 1

Recombinant SNAREs were kindly provided by A.Stein, F.Zilly and T.Siddiqui

2.3. Cell-free assay for exocytosis

2.3.1. Generation of membrane lawns

For preparation of membrane lawns, hNPY-eGFP expressing cells growing on poly-L-lysine coated coverslips were mounted in Plexiglas chamber, which was then filled with 6 ml of ice-cold K-Glu-DPTA buffer (20 mM HEPES-KOH, pH 7.2, 120 mM potassium glutamate, 20 mM potassium acetate, 10 mM DPTA, 2 mM ATP, 4 mM $MgCl_2$, 0.5 mM DTT) and mounted directly on microscope's table. For sonication (Sonifier B12, Branson Ultrasonics Corp., Danbury, CT, USA), a tip diameter of 2.5 mm, a coverslip-to-tip clearance of 10 mm, power setting of 5.5 corresponding to 100 W ultrasonic power delivered to horn tip were used and a duty cycle set setting

"hold" was used as a variable. The sonifier was modified to accommodate a hand trigger for ultrasonic pulse triggering.

Sonicator tip was placed directly above the objective lens and the transfected cells were located. Such cells were exposed repeatedly to a sonication cycles until a membrane lawn or several lawns decorated with secretory granules were generated, as judged by the presence of numerous green fluorescent spots visible in the microscope. This process was monitored throughout its course.

2.3.2. Stimulation of exocytosis

2.3.2.1. Priming and triggering of exocytosis

Membrane lawns were imaged with 500 ms exposures to bring them in focus and to acquire a reference picture. The sonication chamber solution was then carefully exchanged with the K-Glu-DPTA buffer supplemented in various experiments with rat brain cytosol, light chains of clostridial neurotoxins, soluble SNARE proteins, antibodies, α-SNAP (wild-type or L294A), NEM and NSF where indicated. In some series of experiments, ATP and $MgCl_2$ in the K-Glu-DPTA buffer was omitted or replaced by ATP analogues. After 5 min preincubation, the solution was exchanged with K-Glu-DPTA/Ca^{2+} buffer described below. For the 0 μM free Ca^{2+} solutions, K-Glu-DPTA buffer was used. In certain experiments ATP and $MgCl_2$ were omitted or replaced by an ATP analogue as indicated in figure legends. Subsequently, a time-lapse was started and membrane lawns were imaged every 30 s for 15 min using a 500 ms second exposure. Finally, membranes were visualised by adding 50 μl of

saturated aqueous solution of TMA-DPH (1-(4-trimethylammonium)-6-phenyl-1,3,5-hexatriene, Molecular Probes Inc., Eugene, OR, USA) and imaged as described above.

2.3.2.2. Calibration of free calcium used in stimulation buffers

DPTA calcium buffers were calibrated as follows using 10 μM Mag-Fura-2 (Molecular Probes Inc.) ratiometric dye. A standard curve was generated using known concentrations of $CaCl_2$ in calibration buffer (10 mM Tris-HCl, pH 7.2, 100 mM KCl, 0.3 mM $MgCl_2$) produced by serial dilution of a 1 M $CaCl_2$ stock solution. Measurements were performed in a fluorometer (Fluoromax 2, Horiba Jobin Yvon, Munich) with values expressed as a ratio of the emission (510 nm) at two excitation wavelengths – 350 nm and 380 nm at slit settings of 1 nm (excitation) and 2 nm (emission). DPTA and $CaCl_2$ were added to give a working concentration of 10 mM DPTA and calcium in the range of 1-5 mM. DPTA-calcium buffers were prepared in 20 mM HEPES-KOH, pH 7.2, 120 mM potassium glutamate, 20 mM potassium acetate 2 mM ATP, 4 mM $MgCl_2$, 0.5 mM DTT. Fluorescent ratios were determined with reference to the standard calibration curve to define concentration of free Ca^{2+} in the buffer. The effect of cytosol on the free calcium would not be determined due to the resulting strong auto-fluorescence interfering with the measurements. Furthermore, to confirm the results obtained with the ratiometric method, the free Ca^{2+} concentrations were calculated according to (Heinemann et al., 1994) and resulted in similar values as the ones obtained from the standard curve. For

stimulation of exocytosis I used the K-Glu-DPTA buffer containing 3 mM Ca^{2+} to obtain approximately 35 μM free Ca^{2+} in this buffer (referred to as K-Glu-DPTA/Ca^{2+})

2.4. Immunofluorescence and α-SNAP binding-studies

2.4.1. Generation of membrane sheets

Membrane lawns were prepared as described (Avery et al., 2000) except that the K-Glu buffer used for sonication contained DPTA instead of EGTA. These preparations were then used as described.

2.4.2. Immunofluorescence

Before immunostaining of membrane lawns, all antibodies were diluted 200-fold (except for Cl 77.2 that was diluted 400-fold) into PBS (150 mM NaCl, 10 mM Na_2HPO_4, 10 mM NaH_2PO_4, pH 7.4) containing 1% (w/v) BSA and centrifuged for 30 min at 13000 x g_{av}. After sonication, membrane lawns were fixed for 60 – 90 min at room temperature in 4 % paraformaldehyde in PBS, washed with PBS, quenched for 10 min in PBS containing 50 mM NH_4Cl and washed three times in PBS for 10 min each. This was followed by 60 min incubation with primary antibodies. Subsequently, membrane lawns were washed three times in PBS for 10 min each, followed by 60 min incubation with the secondary antibody (goat-anti-rabbit or goat-anti-mouse, Cy3 or Cy5-coupled, Dianova, Hamburg) diluted 1:200 in PBS

containing 1 % BSA. Before imaging, membrane lawns were washed 3 times in PBS for 10 min each and then imaged in a solution containing TMA-DPH to visualize lipid membranes. For imaging, membrane lawns were identified in the TMA-DPH channel and the immunostainings were recorded.

Mouse monoclonal serum against α/β-SNAP (Cl 77.2) was obtained from Synaptic Systems (Göttingen, Germany), mouse monoclonal serum against transferrin receptor was purchased from Zymed (H 68.4, Cat no: 13-6890). Rabbit polyclonal serum against syntaxin 1A (R31, Lang et al., 2001) was used and rabbit polyclonal serum against α-SNAP (R34, raised against His_6-tagged α-SNAP) was generated in the Jahn laboratory.

2.4.3. Binding studies

For binding of α-SNAP, membrane lawns were generated as described above and incubated for 5 min at 37°C in a humid chamber in K-Glu buffer (120 mM potassium glutamate, 20 mM potassium acetate, 20 mM HEPES-KOH pH 7.2) supplemented with α-SNAP (wild-type or L294A variant) recombinant light chains of clostridial neurotoxins, NEM, NSF or rat brain cytosol as indicated. They were then washed with PBS for 10 min, fixed and processed for immunostaining as described above.

2.5. Microscopy and image analysis

2.5.1. Microscopy

All microscopy was performed with a Zeiss Axiovert 100 TV microscope and 100 x 1.4 NA Plan-apochromat objective. Illumination was provided by XBO 75 xenon lamp. Images were acquired using Metamorph 6.1 (Universal Imaging Corp., Downingtown, PA, USA) from a cooled, back-illuminated frame transfer CCD camera (2 x 512 x 512-EEV chip, 13 x 13 µm pixel size or MicroMAX NTE/CCD-512B, 512 x 512 pixel chip, 24 x 24 µm pixel size; Princeton Instruments Inc., Trenton, NJ, USA). To avoid spatial undersampling by the large pixels a magnifying lens (1.6 x or 2.5 x Optovar) was used during imaging. The focal position of the objective was controlled throughout all experiments using a low voltage piezoelectric translator driver and a linear variable transformer displacement sensor/controller (Physik Instrumente, Waldbronn, Germany).

eGFP fluorescence was detected using Chroma filter set F41-054 (excitation filter HQ 480/40, dichroic mirror Q505LP, emission filter HQ 527/30). Cy3 fluorescence was detected with Chroma filter set F41-004 (excitation filter HQ 560/55, dichroic mirror Q595LP, emission filter HQ 645/75). Cy5 fluorescence was detected with Chroma filter set F41-008 (excitation filter HQ 700/75, dichroic mirror Q660LP, emission filter HQ 620/60). TMA-DPH fluorescence was detected using Chroma filter set F11-000 (excitation filter D 360/50, dichroic mirror 400DLP, emission filter E 420 LP). All filter sets were provided by AHF Analysentechnik (Tübingen, Germany).

2.5.2. Image analysis

2.5.2.1. Quantification of immunostaining

For comparative quantification of α-SNAP immunoreactivity, membrane sheets were identified in the TMA-DPH pictures, each containing up to 30 individual membrane sheets. Up to 20 areas of ~9 – 16 μm^2 each covering several dozens of stained fluorescent spots were placed randomly on membrane sheets and then transferred to the Cy5-channel with corrections being made to avoid obvious artifacts such as highly fluorescent contaminating particles that were occasionally seen. In each area, the overall fluorescence intensity was quantified. Local background was measured in an area outside the membrane sheets and subtracted. For each condition, 100 – 200 membrane sheets per experiment (mean – 120) were analyzed and the mean was calculated. Each experiment was performed independently 3 - 6 times. Values are given as mean ± SEM.

2.5.2.2. Co-localization

To determine co-localization of spots in two channels, we used a procedure previously described (Lang et al., 2002). Circles were centered on randomly selected individual spots (up to 200 each per individual membrane sheet) in one channel and then transferred to the second channel. If the fluorescence intensity maximum of a corresponding spot in the second channel was within 2 pixels of the spot in the first channel, it was rated as co-localized. To correct for accidental co-localization, the

image of the first channel was superimposed with a mirror image of the second channel, and co-localization was determined as above. Background correction was performed according to the following formula: real co-localization = (measured co-localization – background co-localization)/(1 – background colocalization/100). For each experimental condition, we analyzed at least 10 individual membrane sheets Values are given as mean ± SEM. Values obtained for α-SNAP/syntaxin were 58 % ± 2 and for α-SNAP/transferrin receptor 9 % ± 2.

2.5.2.3. Determination of exocytotic activity

During an *in vitro* exocytosis experiment a stack that consists of 35 image planes stored as .tif files is acquired and used for analyses. The first picture taken is the image acquired immediately after a lawn has been generated, another one after the 5 min-long pre-treatment stage. These first two planes serve only as reference pictures to verify that no secretory granules detaches from membrane during the preincubation phase. Acquisition time totals 15 min with two, 500 ms-long exposures per minute. At the end of 15 min-long time-lapse another two reference pictures are acquired. The penultimate plane is a picture of the so-called background image. This picture of offset noise is later subtracted from all other planes in the stack. Due to the fact that, the thermal noise build-up can be pixel-dependent this motivates the subtraction of a whole image rather than a single mean value of the entire picture.

The final plane is a picture of membrane lawn labelled with unspecific lipid dye TMA-DPH. That image serves as an ultimate verification of membrane lawn's shape

and integrity. Finally, remaining 33 planes (without two first reference planes) are used for analyses performed with Cantata Khoros software (Khoral Inc., Albuquerque, NM, USA).

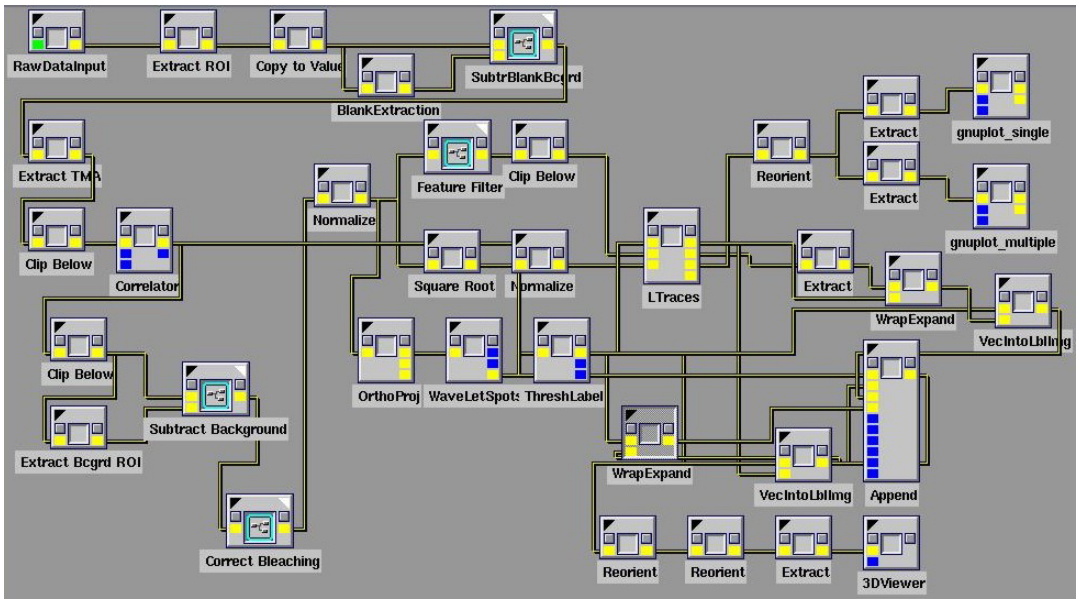

***Figure 5* – Scheme of Cantata workspace used for analyzing microscopic stacks of pictures acquired during experiments.**

All these planes are fed in the program by its first procedure called “raw data input”. By comparing images from the TMA-DPH and GFP channels a suitable region of interest (ROI) was selected. This ROI is extracted from all 33 planes, with the aim of faster data evaluation. This reduces the size of data set to be processed by the program. The background picture is subsequently subtracted from each plane of the stack. After the subtraction, this plane is removed from analysis leaving the stack with 31 planes (+ the TMA-DPH). TMA-DPH plane is also removed during next step

of analysis what produces ultimately 31 planes that would enter the main analysis scheme.

After correction some pixels might have negative values due to the sporadic presence of so-called “hot pixels” giving rise to unusually high pixel values. The “clip below” procedure replaces negative data values what prevents the program from stopping during next routines. In this case all negative values are set to minimal positive value of one.

Normally, the planes acquired by microscope camera display various levels of shift between consecutive pictures. This is caused by mechanical vibrations of microscope table due to manipulations during the experiment. In order to analyze any stack of pictures to precisely determine fates of individual granules, one must align them in the lateral dimensions to correct for these shifts. The “correlator” routine corrects for lateral drifts which occur during acquisition. Correlator is based on maximizing the cross-correlation between two planes. The first plane out of 31 entering the program serves as a reference plane to which all other planes are aligned. In three iteration steps it tries to find the maximum cross-correlation with a centre-of-mass based algorithm.

Local background signal around membrane lawn is corrected by the “extract background ROI” routine. It allows the user to select a small region of background outside the membrane lawn, the mean value of which will later be subtracted from the entire stack. All pixel values are normalized to minimal and maximal values in the stack of pictures to replace the original signal dynamics with values 0 – 100.

To identify objects on membrane lawn as granules or non-granules the program had to define to what spatial frequencies granules would correspond to. This process was be aided by fast Fourier transforms. Certain spatial frequencies present in the original pictures were suppressed in the processed output image. A side-effect of this filtering could be seen as dimmer rings around more brightly delineated granules. After completion of Fourier space operations for all planes, data was averaged along the time dimension (i.e. consecutive planes in the stack) for each pixel to form an overview image used for segmentation.

Additional signal-enhancement routines e.g. “wavelet spots” (Olivo-Marin, 2002) were applied through the course of analysis. Subsequently, the images were labelled by “threshold label” routine using a fixed thershold. Ultimately, final step of analysis – “label traces” routine is applied. It performs the classification of granules’ types and their behaviours based on the Fourier-filtered image and the label-identification image (which pixel belongs to which object number).

A scheme clarifying logics behind automated classification performed by the program is presented in the following figure.

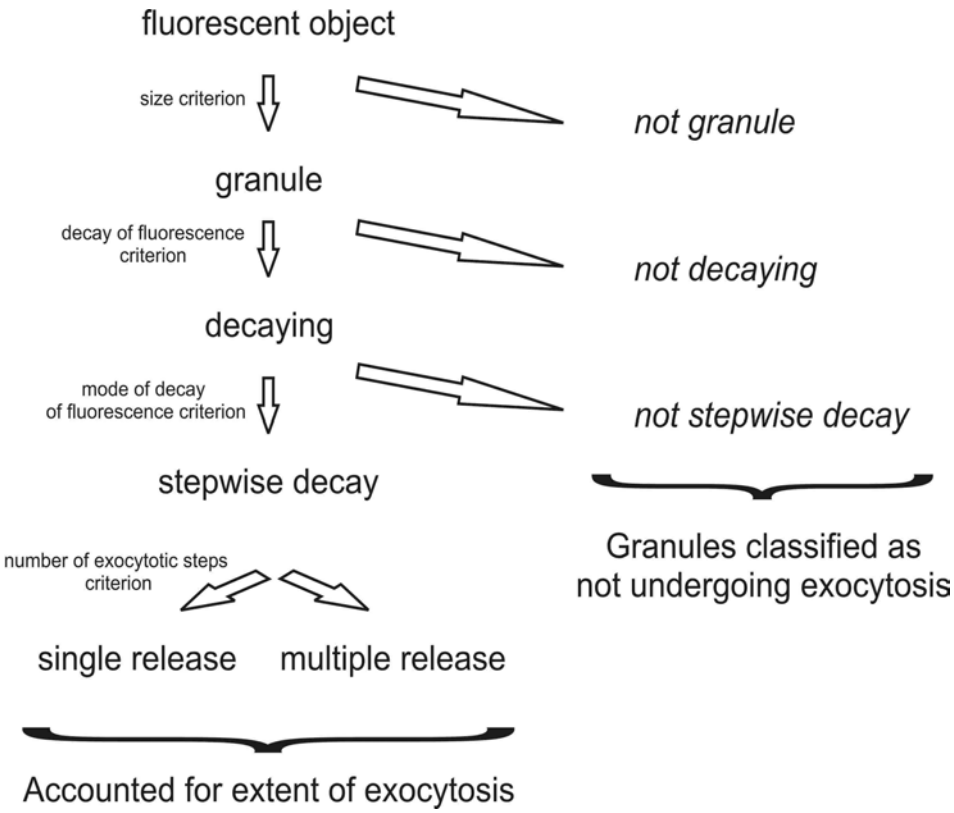

***Figure 6* – Flowchart of Cantata logics applied for analyzing and classifying exocytosis from secretory granules.**

Here an object is defined to be a granule when it fulfils basic criteria:

- Its size must be between 4 pixels and 20 pixels to be considered as a “valid” granule. If this criterion is not fulfilled, it led to its exclusion from the statistics and classification as "invalid".

- The “valid” objects are further classified into two categories – "**exocytosed**" and "**non-exocytosed**".
    - Exocytosed objects are ones which lost at least 60% of their intensity during 15 min of recording and which exhibited at least one and 25% stepwise drop (or “gap”) in intensity of fluorescence that occurred between two consecutive frames.
    - These objects are further divided into two last categories of “**single events**” and “**multiple events**”.

      The single events are characterised by a single, frame-to-frame (i.e. stepwise) loss of intensity of fluorescence. The multiple events are the ones that have more than one detected gap but they are counted as one exocytotic event.

Exocytotic activity was expressed as number of exocytotic events divided by number of objects classified as granules. For evaluation of the program’s accuracy and reliability in assignment of exocytotic mode to granules on the picture I have compared the program output with manual way of analysing the data. This enabled a comparison for estimating errors and/or omissions made either way of analysing the data sets. The comparison showed that either analysis led to omissions and mis-assignments, however, the errors were in the range of 1,6 % for the program output verified manually and 1,1 % for the manual assignment verified later by Cantata. This allowed for concluding that the automated analysis was reliable for scoring exocytosis occurring in the assay presented here.

2.6. Other methods

2.6.1. Preparation of rat brain cytosol

Cytosol was prepared according to Martin, 1989. Brains (without the cerebella and brain stems) of 40 freshly killed male Wistar rats were placed into 40 ml ice-cold isotonic buffer (130 mM NaCl, 2 mM EGTA, 50 mM PIPES, pH 7.0, 0.1 mM PMSF supplemented with protease inhibitor cocktail (Complete, Roche, Mannheim, Germany)) and homogenised with one slow and three fast strokes of a Teflon homogeniser running at 800-1000 rpm at 4°C. Larger debris was removed by centrifugation at 14500 x g_{av} (SS-34 rotor, Sorvall) for 15 min at 4°C. The supernatant was collected and centrifuged at 128000 x g_{av} (TLA 100.3 rotor, Beckman Coulter, Krefeld, Germany) for 60 min, 4°C to remove myelin and mitochondria. The second supernatant was then dialysed (dialysis tubing – molecular weight 6000-8000 Da cut-off) into 1 litre of ice cold K-Glu buffer for 4 hr at 4°C. Buffer was exchanged every hour. Cytosol was then aliquoted, snap-frozen in liquid nitrogen and stored at -80°C. Protein concentration was determined by Bradford assay.

2.6.2. Bradford assay - determination of protein concentration

Protein concentration was determined by the Bradford assay. 1 µl rat brain cytosol was diluted 1:2, 1:5, 1:10 in ddH_20 to give final volume of 2, 5, 10 µl of diluted and 1 µl of un-diluted cytosol. Each of these were diluted to final volume of 200 µl with

ddH_2O in 1.5 ml Eppendorf tubes and centrifuged at 16000 x g_{av} for 3 min in a bench top centrifuge (Biofuge Fresco, Heraeus). Samples were transferred to new tubes and 800 µl of Bradford reagent (BioRad) was added followed by incubation for 5 min at RT. Absorbance of samples was measured at 595 nm and the concentration determined from values for a BSA standard curve prepared from 0.5 to 20 µg BSA diluted in ddH_2O from 0.01 % of BSA stock solution. Typically, concentration of rat brain cytosol proteins was in a range of 10-15 mg/ml

2.6.3. Plasmids

The plasmid encoding a fusion protein of human neuropeptide Y (Lang et al., 2001) with eGFP was used. The plasmid DNA was transformed into *E. coli* XL-1 blue bacteria (Stratagene, Heidelberg, Germany), isolated from overnight cultures of grown from a single colony of transfected cells, using the Qiagen Giga systems according to the manufacturer instructions. Purified plasmid was re-suspended in TE buffer (10 mM Tris-HCl, pH 8.0, 1 mM EDTA) or ultra pure water. For determination of DNA concentration, small volumes of DNA suspension were diluted 1:50 and 1:100 in TE buffer or water to photometrically determine concentration (10 mm path-length Quartz cuvette, Genequant photometer, Pharmacia Biotech). Plasmid DNA was then stored at -20°C.

3. Results

3.1. Improved cell-free assay for exocytosis in PC12 cells

As outlined in the introduction, in the laboratory of Reinhard Jahn, a cell-free assay for exocytosis based on the generation of membrane lawns containing fluorescent, docked secretory granules that are imaged during exocytosis has been developed. In the present work, two aspects of this assay: (1) reduction of the time delay between ultrasonic rupture of a cell and the priming/triggering of the fusion and (2) automated analysis and scoring the rate of exocytosis have been established.

3.1.1. On-stage sonication of PC12 cells and stimulation of exocytosis *in vitro*

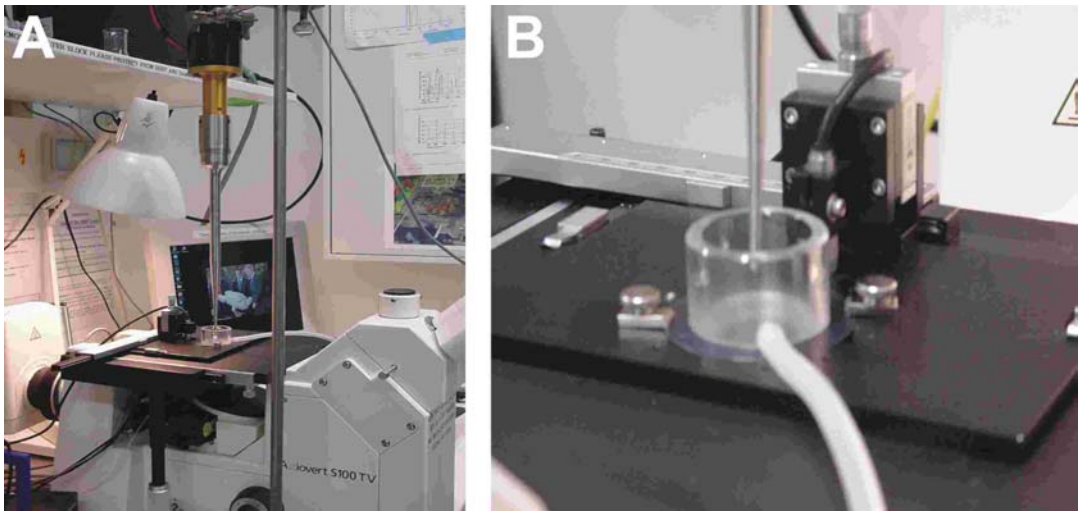

***Figure 7* – (A) Photograph of the microscopic setup used for on-stage sonication of PC12 cells. (B) Close-up of a Plexiglas sonication chamber with cells-bearing**

glass coverslip on the bottom of it and titanium sonication tip pointing into the chamber's lumen.

For preparation of membrane lawns, hNPY-eGFP expressing cells grown glass coverslips were mounted in Plexiglas chamber, which was then filled with 6 ml of ice-cold K-Glu-DPTA buffer (20 mM Hepes, pH 7,2, 120 mM potassium glutamate, 20 mM potassium acetate, 10 mM DPTA, 2 mM ATP, 4 mM $MgCl_2$, 0,5 mM DTT) and mounted directly on microscope's table. Sonicator tip was placed directly above the objective lens and transfected cells were located. Such cells were exposed repeatedly to a sonication cycles until a membrane lawn or several lawns decorated with secretory granules were generated, as judged by the presence of numerous green fluorescent spots visible in the microscope. This process was monitored throughout its course.

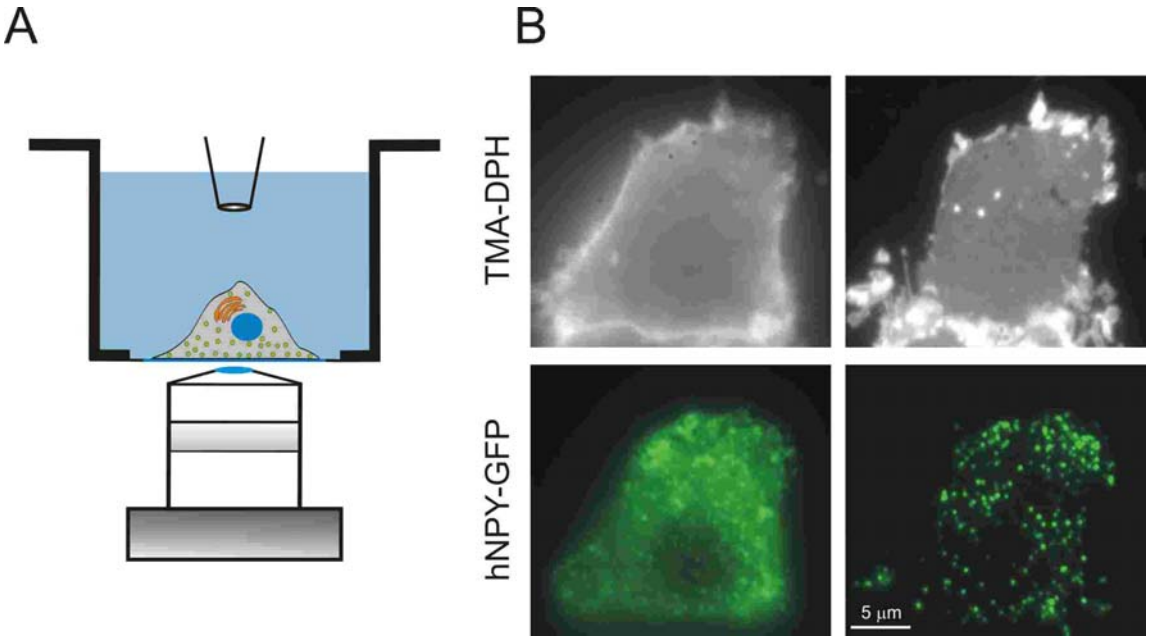

◄ Previous page, *Figure 8* – (A) Scheme of experimental setup of the cell-free assay exocytosis. (B) Visualization of eGFP-expressing PC12 cells before and after ultrasonic disruption.

(**A**) Sonication of PC12 cells grown on coated coverslips is carried out atop the microscope in a small chamber and the entire process can be monitored on-line throughout its course. (**B**) This treatment created flat membrane lawns decorated with LCDVs labelled with human neuropeptide Y coupled to eGFP (hNPY-eGFP, lower panel). The hNPY-eGFP-expressing PC12 cells produced flat, two-dimensional membrane fragments with green LDCVs attached onto them. Membrane lawns were stained by an unspecific lipophillic dye TMA-DPH (upper panel).

Membrane lawns were imaged to bring lawn in focus and to acquire a reference picture. The sonication chamber solution was then carefully exchanged with the K-Glu-DPTA buffer supplemented in various experiments with rat brain cytosol, light chains of clostridial toxins, soluble SNARE proteins, antibodies, α-SNAP (wild-type or L294A), NEM and NSF where indicated. In some series of experiments, ATP and $MgCl_2$ in the K-Glu-DPTA buffer was omitted or replaced by ATP analogues. After 5 min preincubation, the solution was exchanged with K-Glu-DPTA/Ca^{2+} buffer described below. For the 0 μM free Ca^{2+} solutions, K-Glu-DPTA buffer was used. In certain experiments ATP and $MgCl_2$ was omitted or replaced by an ATP analogue as indicated in figure legends

3.1.2. Imaging exocytotic release in the cell-free assay

Exocytosis of green-labelled large, dense-core vesicles was judged from abrupt dimming of green eGFP content of granules. This loss of fluorescence corresponded to release, and often complete loss of vesicle's cargo what was monitored on-line by fluorescence microscopy at a single granule level.

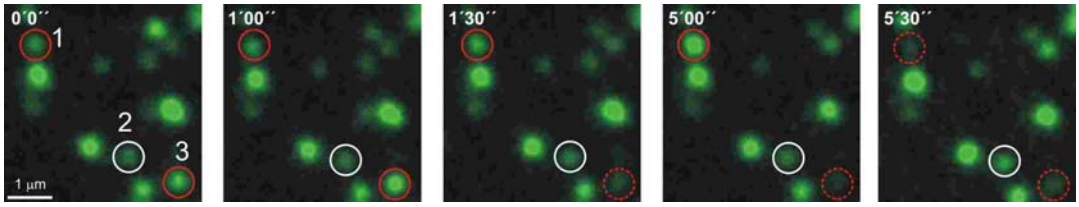

Figure 9 **– Monitoring of membrane fusion by fluorescence microscopy.**

Secretory granules labelled by expression of the secretory vesicle marker hNPY-GFP were attached to membrane lawns. They were first incubated for 5 min in K-Glu-DPTA buffer which was replaced thereafter by K-Glu-DPTA supplemented with 3 mM $CaCl_2$ (K-Glu-DPTA/Ca^{2+} resulting 35 µM free Ca^{2+}) to trigger exocytosis at t=0 (for details please refer to **Methods**). Images were acquired every 30 s for 15 min, and the changes of granule fluorescence intensity over time were measured. Red circles depict granules that underwent abrupt loss of GFP between consecutive frames. White circle indicates a granule that did not undergo exocytosis within the time lapse recorded.

In some instances, eGFP fluorescence increased prior to its loss what could be best explained by its quenching at low pH. When a fusion pore is formed the interior of vesicle is subjected to pH change from acidic ~5,5 to neutral of approximately 7,0 –

7,5. This rise in pH has been shown to increase by 50 % intensity of GFP stored inside vesicle (Patterson et al., 1997). Such rise is then followed by a dilation of the fusion pore and a release of vesicle content resulting in dimming of granule and GFP diffusion out under the cell membrane.

3.1.3. Quantification of exocytotic activity

To quantify the observed exocytosis initiated after application of Ca^{2+}, a semi-automated way of analyzing the data has been designed. Scoring of exocytosis was performed with Cantata software (Khoral Inc., Albuquerque, NM, USA). Microscopic images were corrected for unspecific noise originating from the camera and the surroundings of a membrane lawn, corrected for lateral shifts and analyzed with fast Fourier transforms-based procedures to yield a number of granules undergoing exocytosis on the membrane lawns. As described in details in the **Methods** section, exocytotic activity was expressed as number of exocytotic events divided by number of objects classified as granules. For evaluation of the program's accuracy and reliability in assignment of exocytotic mode to granules on the picture, the program's output was compared with the outcome of manual analysis of the data. This enabled a comparison between Cantata-processed images with an evaluation in MetaMorph to estimate errors and/or omissions made either way of analyzing the data sets.

3.1.4. Application of changes in fluorescence for analysis of exocytotic events

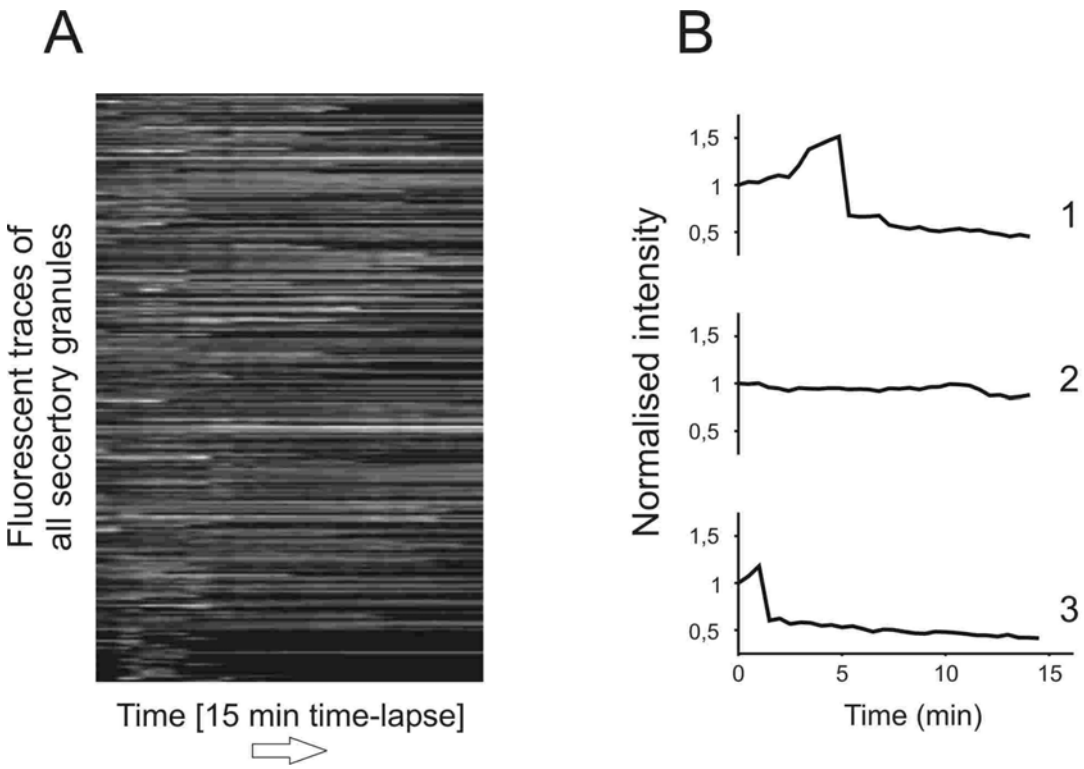

***Figure 10* – (A) Exemplary intensity traces of all granules from one lawn that was triggered with calcium to exocytose. White lines indicate changes of fluorescence of granules over time. Points where bright lines end, likely represent fusion of vesicle and emptying of its content as judged by the disappearance of the eGFP label. (B) Exemplary intensity traces of secretory granules shown in Figure 9. Intensity values were corrected for local background, normalized to the initial intensity and plotted against time.**

Most exocytotic events recorded with use of the improved *in vitro* system exhibited either (1) an increase in intensity of fluorescence followed by an abrupt loss of it, or (2) an abrupt loss without preceding increase, as the GFP diffused out of a vesicle. Increase in fluorescence intensity before its abrupt intensity loss (e.g. granule **1** in

Figure 9 and **Figure 10 B**) could be ascribed to a population of granules that formed a fusion pore which firstly permitted for pH neutralization and stayed opened for a period of time to then allow for eGFP release from vesicle interior (Holroyd et al., 2002). Such a change in fluorescence intensity prior to release would not always be recorded due to low image acquisition frequency during the time-lapse recording in my assay. Acquisition of images at higher frequency was not possible because of very strong photodamage of eGFP and resulting "bleaching" of the dye what prevented from faster imaging.

These two types of exocytotic events occurring in my assay, referred to as "$F_{up+down}$" and "F_{lost}", by Holroyd and colleagues, were classified as "exocytosed" and included in the final analyses of activities – see the above Cantata logics flowchart in **Figure 6**.

3.2. Characterisation of the exocytotic responses in the improved cell-free assay.

I tested various preincubation times followed by Ca^{2+}-triggering and concluded that 5 min-long preincubation did not change the exocytotic response (data not shown). The exocytotic activity measured afterwards was not different from the observed on lawns triggered immediately without the preceding preincubation. This observation allowed for setting interval of 5 min as an optimal time window for preincubation in all *in vitro* exocytosis experiments and in majority of α-SNAP binding studies presented in later sub-chapters of the **Results** part. All data pertaining to the exocytotic activity and presented in this section reflect activity that was recorded during 15 min of a time-lapse acquisition. Time resolution of these experiments was not performed due to often low number of the exocytotic events per unit time (30 s intervals between image acquisitions). This might have led to unclear and large error-bearing division of exocytosis into faster and slower phase and was not performed.

In addition, all activity data values presented below were not corrected for unspecific, Ca^{2+}-indpendent background activity, i.e. negative control which was always in the range 8-10 %.

3.2.1. Cytosolic factors seem to modulate exocytosis differently in the presence of ATP-Mg.

Important role of cytosol in priming processes has been demonstrated in various cell-free systems. To test the cytosol dependence of my assay, series of experiments were performed that involved treatment of the membrane lawns with cytosol in conjunction with ATP-Mg or in the absence of it.

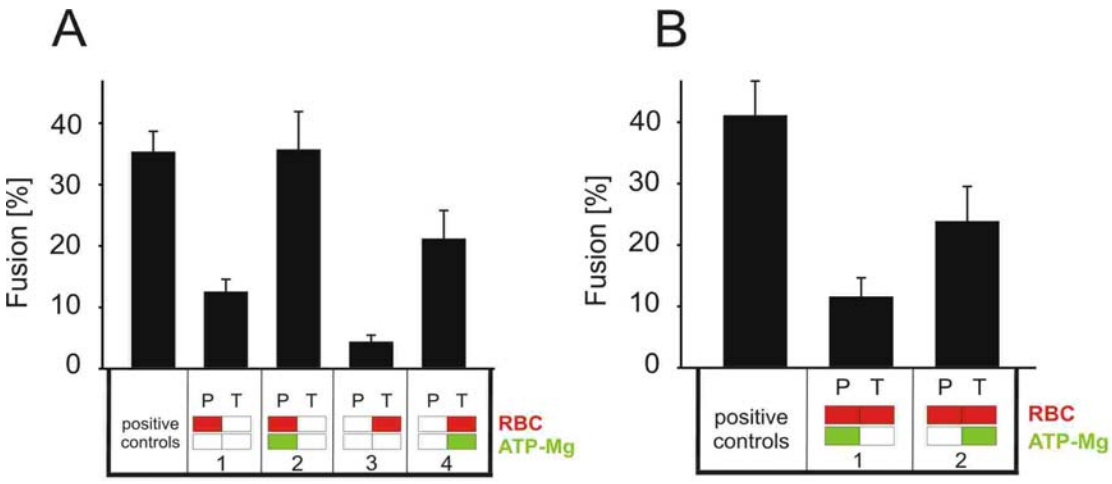

***Figure 11* – ATP-dependence of the cell-free assay is modulated upon addition of rat brain cytosol**

Exocytosis of LDCVs is dependent on ATP-Mg and can be modified by cytosol present during preincubation and/or stimulation. Fusion of secretory granules was triggered as described in **Methods**. Briefly, K-Glu-DPTA buffer used for the preincubation (**P**) and K-Glu-DPTA/Ca^{2+} buffer used for triggering (**T**), contained ATP (indicated in green) and/or rat brain cytosol (RBC, indicated in red). In certain experiments ATP-Mg and RBC were omitted what is indicated as white rectangles in the figure. The values of the exocytotic activities were not corrected for a background activity, i.e. negative control

that was always in the range 8-10 %. All values are expressed as mean ± SEM. n = 5 – 11 membrane lawns per condition. Each lawn was treated as an independent "single-cell" experiment.

The positive control activity on fully primed (i.e. ATP present in the preincubation and the triggering stages) and Ca^{2+}-triggered membranes was as usual in a range 30 – 40 %, whereas primed but not Ca^{2+}-triggered lawns (negative control) typically exhibited 8 – 10 % activity (not shown in the figure). When the preincubation or the triggering buffers contained only cytosol (ATP-Mg was omitted) exocytosis was reduced to 12,5 % ± 2,0 and 4,3 % ± 1,1 (**Fig. 11 A-1** and **A-3**, respectively). Application of ATP-Mg in conjunction with cytosol caused interesting effects. When cytosol was present together with ATP-Mg during the preincubation stage (**Fig. 11 A-2**), the exocytosis did not decrease – 35,6 % ± 6,2 – as observed for the condition without RBC (see **Fig. 12-3** – 21,8 % ± 4,4). Similar to this effect, when ATP-Mg and cytosol were absent from the preincubation stage but were both introduced in the triggering phase (**Fig. 11 A-4**), they seemed to prevent severe run-down of activity and exocytosis accounted for 21,1 % ± 4,6 (compare with **Fig. 12-4** – no ATP-Mg in the priming stage – 8,5 % ± 1,5).

In another experimental series (**Fig. 11 B**), cytosol was present throughout the course of experiment whereas ATP-Mg was introduced only in the preincubation (**Fig. 11 B-1**) or the triggering stage (**Fig. 11 B-2**).

In contrast to result shown in **Fig. 11 A-2**, this treatment resulted in a strong decrease of exocytotic activity to 11,5 % ± 3,0 when only the preincubation buffer contained

ATP-Mg. This decrease in exocytosis was not seen when ATP-Mg was present in the triggering buffer and activity remained on a relatively high level of 23,8 % ± 5,6 (**Fig. 11 B-2**).

In contrast to earlier studies performed in permeabilized PC12 cells (Hay and Martin, 1992), cytosol was not a limiting factor in my assay and was not required for efficient Ca^{2+}-triggered exocytosis. The crucial factor for the triggering was ATP-Mg. To address the question of its importance for fusion in my assay, series of experiments presented in the next sub-chapter was performed.

3.2.2. Exocytosis on membrane lawns is strictly dependent on ATP-Mg.

The importance of ATP in the exocytotic pathway has been demonstrated in many assays and is undisputable in light of experimental results (Hay and Martin, 1992). However, as discussed in the **Introduction** chapter, ATP-Mg-dependent steps are not precisely mapped and despite understanding of some of these reactions, the exact role and order of energy-requiring stages remain unclear.

Results of the experiments involving cytosol and ATP-Mg that showed lack of cytosol dependence led to addressing the questions of effects caused by ATP-Mg in my cell-free assay.

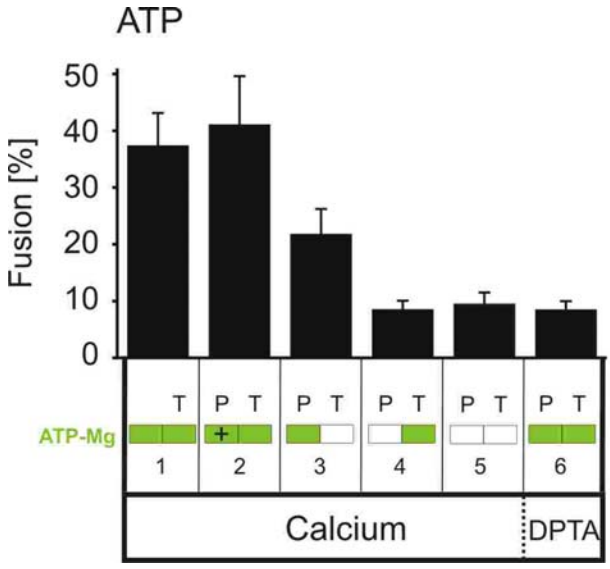

***Figure 12* – ATP-Mg is required in the assay throughout the course of experiment in order to maintain fusion on isolated membranes.**

Effects of ATP-Mg presence during preincubation and/or stimulation on exocytosis of secretory granules. Fusion of secretory granules was triggered as described. Solutions used in the preincubation (**P**) or the triggering (**T**) contained ATP-Mg (indicated in green). Under some experimental conditions ATP was omitted from either buffer. In series of experiments the concentration of ATP-Mg in the preincubation buffer was raised from standard 2 mM to 20 mM what is indicated with "**+**" in the figure. In a negative control experiment buffer used for the triggering was K-Glu-DPTA. All values are expressed as mean ± SEM. n = 8 – 12 membrane lawns per condition.

When ATP was present at 2 mM concentration during the preincubation and the triggering phase (positive control), Ca^{2+}-induced exocytosis reached 37,3 % ± 5,7 (**Fig. 12-1**). Removal of ATP-Mg from the preincubation phase very strongly reduced exocytosis to 8,5 % ± 1,5 (**Fig. 12-4**). On the other hand, when ATP-Mg was present during the preincubation but not the triggering phase (**Fig. 12-3**), exocytosis was also reduced, however, to a much lesser extent accounting for 21,8 % ± 4,4 of fusion. Withdrawal of ATP-Mg from both experimental stages (**Fig. 12-5**) resulted in virtually complete block of exocytosis and its reduction to 9,5 % ± 2,0. This value is comparable with negative control activity – 8,4 % ± 1,5 obtained after triggering fusion with K-Glu-DPTA buffer (**Fig. 12-6**). In other series of experiments I tried to saturate the priming reactions with excessive amounts of ATP-Mg (**Fig. 12-2**). When concentration of ATP-Mg was elevated 10-fold from 2 mM to 20 mM, no significant increase in exocytosis was observed (41,1 % ± 8,5).

The presence of ATP-Mg was required for Ca^{2+}-dependent exocytosis what is in agreement with previous observations made in permeabilized cells (Hay and Martin, 1992; Holz et al., 1989). In the experiments that followed two series presented above, I tested in my assay analogues of ATP to disturb ATP-Mg-requiring processes and to better characterize the nature of ATP-Mg-dependent responses.

3.2.3. Various ATP analogues do reduce exocytosis when introduced in two-stage assay.

In order to further investigate ATP-Mg dependence I decided to take advantage of known ATP analogues that have been reported to block exocytosis in patch-clamped chromaffin cells (Xu et al., 1998). These reagents cannot be hydrolyzed by ATPases or by kinases inducing massive inhibition of most, if not all, ATP-Mg-requiring steps. Both ATPγS and AMP-PNP were used in my cell-free system to test whether in an acutely prepared membrane lawn assay they inhibit exocytosis as reported previously.

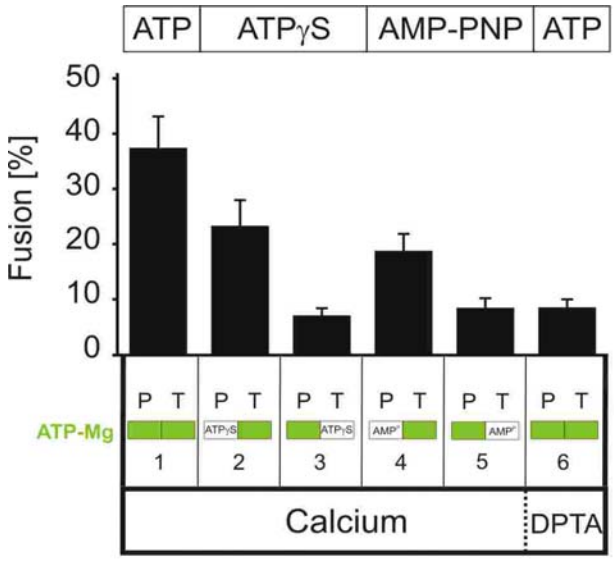

***Figure 13* – Fusion in an *in vitro* exocytosis assay is inhibited most potently when ATP analogues are introduced in the triggering phase.**

Effects of application of non-hydrolysable analogues of ATP during the preincubation and/or the stimulation phases on exocytosis of secretory granules. Fusion of granules was triggered and measured as described. The

preincubation (**P**) or the triggering (**T**) solutions contained ATP-Mg (indicated in green). As indicated, in some experimental conditions, ATP-Mg was omitted and replaced by its analogues - ATPγS or AMP-PNP. In a negative control experiment buffer used for the triggering was K-Glu-DPTA. All values are expressed as mean ± SEM. n = 7 – 11 membrane lawns per condition.

Control membrane lawns were preincubated and stimulated as described. This triggered exocytosis that reached 37,3 % ± 5,7 (**Fig. 13-1**). When triggering was performed with K-Glu-DPTA buffer, background exocytosis reached approximately 8 % (**Fig. 13-6**), similar to the value shown in the previous figures.

ATPγS introduced in the preincubation but not the triggering phase (**Fig. 13-2**) reduced exocytosis to 23,2 % ± 4,6, when added in reverse order, the inhibition was more pronounced and reaching 7,0 % ± 1,3 (**Fig. 13-3**).

A very similar pattern of responses was observed for the other analogue, AMP-PNP. Exocytosis was decreased to 18,7 % ± 3,1 when AMP-PNP was present during the preincubation (**Fig. 13-4**). When introduced in the triggering phase, the AMP-PNP-induced inhibition reached 8,4 % ± 1,7 (**Fig. 13-5**) what is in the range of negative control and value obtained after ATPγS treatment in the corresponding experiment.

Both analogues of ATP inhibited fusion in my assay. This observation corroborates the notion that the presence of ATP-Mg was required for Ca^{2+}-dependent exocytosis in this exocytosis assay.

3.2.4. SNARE-specific clostridial toxin light chains reduce exocytosis in cell-free assay.

One of the questions addressed with my assay concerned the state of the SNARE proteins residing in freshly prepared lawns. Probing the nearly-native SNAREs exposed on the inner side of cell membrane with respective light chains of clostridial toxins could shed some light on the status of SNARE proteins. Results from these experiments performed are shown in the next figure.

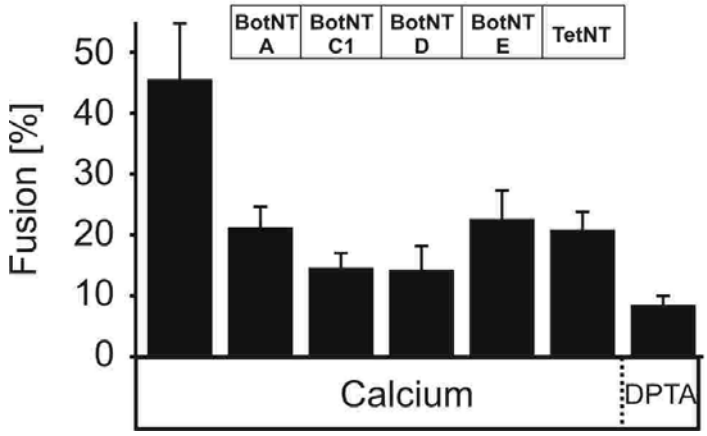

Figure 14 **– SNARE-specific clostridial neurotoxins reduce activity on membrane lawns.**

Various recombinant light chains of clostridial neurotoxins were delivered to membrane lawns in the preincubation buffer. Toxins light chains' concentrations were in the range of 1 – 10 μM. Their activities were previously tested on recombinant SNARE proteins or proteoliposomes incorporating them. Fusion was triggered as described. In the positive control experiments membrane lawns were not preincubated with any toxin light chain but bovine serum albumin was included instead. Both the preincubation

and the triggering buffers contained ATP-Mg. In a negative control experiment buffer used for the triggering was K-Glu-DPTA. All values are means ± SEM. n = 5 – 10 membrane lawns per condition

Treatment with toxins reduced fusion of secretory granules with the plasma membrane by approximately 50 % of overall activity and the strongest reduction was observed for BoNT C1 and BoNT D – to 14,6 % ± 2,3 and 14,2 % ± 3,9, respectively (**Fig. 14**). BoNT A reduced exocytosis to 21,2 % ± 3,4 what closely resembles result obtained in adrenal chromaffin cells (Xu et al., 1998) where this toxin did not completely abolish release but slowed it down. Treatment of lawns with BoNT E brought virtually identical outcome – reduction of exocytosis to 22,6 ± 4,6 %. Experiments with tetanus toxin (TeNT) showed that similar to other toxins tested, it reduced exocytosis to similar value of 20,8 % ± 2,9.

It could be shown, that all clostridial neurotoxins' light chains strongly reduced Ca^{2+}-dependent exocytosis in the cell-free assay. The extent of toxin-induced removal of SNAREs was dependent on a serotype of toxin and reflected their specificity towards the respective SNARE proteins.

3.2.5. Anti SNAP-25 antibody (71.1) inhibits fusion only after extended preincubation. Soluble domains of Q- and R-SNARE proteins inhibit exocytosis on membrane lawns.

Antibodies against SNAREs or SNARE-related proteins have been applied in many experiments to probe the status of these molecules and to perturb their function (Xu et al., 1999). In the current study I decided to use the anti-SNAP-25 (Cl 71.1) antibody to address the question of SNAP-25 availability. In addition, series of experiments involving application of soluble domains of SNARE proteins were performed.

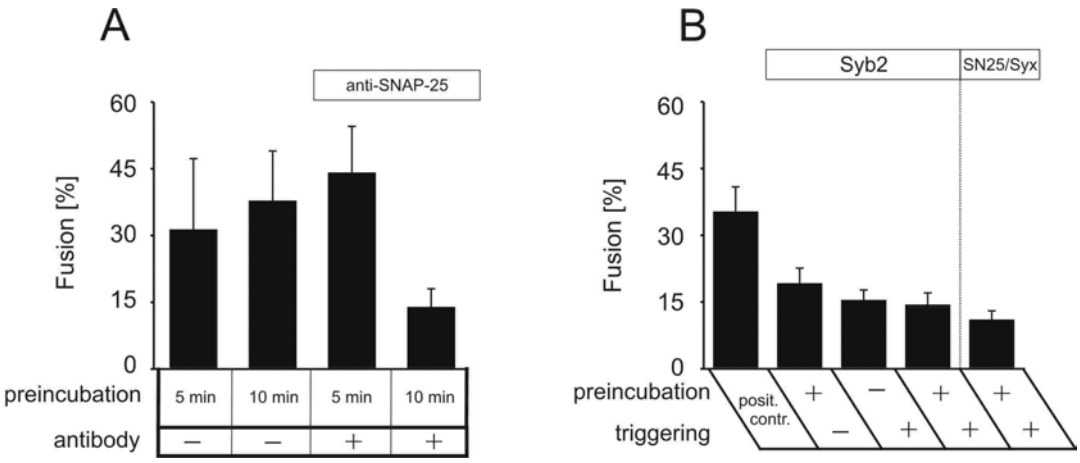

***Figure 15* – (A) Anti-SNAP25 antibody (Cl 71.1) does not block exocytosis after 5 min preincubation, however it reduces fusion strongly after additional 5 min of incubation. (B) Soluble domains of Q- or R-SNAREs reduce exocytotic activity when administered during the preincubation or the triggering phase of experiment.**

The Cl 71.1 antibody was dialyzed against K-Glu-DPTA buffer and applied at approximately 2,5 μM concentration. Recombinant SNARE were diluted in K-

Glu-DPTA (the preincubation buffer) or K-Glu-DPTA/Ca^{2+} (the triggering buffer) without prior dialysis. Synaptobrevin 2 was used at a concentration of 10 μM, whereas SNAP-25 and syntaxin 1a were applied at 2,5 μM and 250 nM, respectively. Positive control experiments, depicted as leftmost bars on both graphs were performed in the absence of cytosol, SNAREs or antibodies but in the presence of BSA in amounts corresponding to concentration of these factors. In a negative control experiment (not shown), buffer used for the triggering was K-Glu-DPTA. All values are means ± SEM. n = 6 – 13 membrane lawns per condition.

Co-incubation of freshly prepared membrane lawns with a monoclonal antibody against SNAP-25 (Cl 71.1) for 5 min at 2,5 μM concentration did not have impact on fusion (**Fig. 15 A**). The exocytotic activity was not reduced when compared to positive control. However, prolongation of antibody treatment reduced activity by approximately 70 % from 44,1 % ± 10,4 to 13,9 % ± 4,1 without apparent reduction of activity in a 10 min-preincubated control experiment.

Lawns incubated with the R-SNARE, synaptobrevin 2, exhibited similar degree of exocytosis inhibition between conditions differing in Syb 2 presence during the preincubation, the stimulation or during both phases of experiment (**Fig. 15 B**). In comparison to a positive control (35,3 % ± 5,5), synaptobrevin 2 reduced fusion to a range between 19,1 % and 14,3 %. The strongest effect was observed upon addition of Q-SNARES – SNAP-25 and syntaxin 1a which were present throughout the entire experiment. In this case exocytosis on lawns was reduced 11,0 % ± 1,9. Negative control (background) activity was in the usual range of 9 % (not shown).

Both molecular tools used in these series of experiments inhibited exocytosis on membrane lawns. Prolonged action of an antibody and addition of the recombinant SNARE proteins likely perturbed assembly of the SNARE complex and thereby reduced exocytosis.

3.3. The α-SNAP inhibits exocytosis in the *in vitro* assay.

I demonstrated that in the assay presented here rat brain cytosol was not required. Such lack of dependence of the system on cytosol differs from noradrenaline release in permeabilized PC12 cells, which is reduced upon omission of cytosol (Hay and Martin, 1992). On the other hand, Ca^{2+}-dependent exocytosis required the continuous presence of ATP-Mg what is in agreement with previous observations on permeabilized cells.

I asked whether ATP-Mg-dependence reflects NSF-driven disassembly of the "*cis*"-SNARE complexes as a prerequisite for exocytosis. It has been previously shown that SNAREs are uncomplexed and active in freshly prepared membrane lawns (Lang et al., 2002), raising the possibility that SNARE disassembly may not be rate-limiting under conditions present in my assay. Previously observed lack of cytosol dependence suggested that NSF and α-SNAP, both soluble proteins, are not required in this system. However, it is possible that small amounts of both proteins are retained on membranes, what would perhaps suffice to disassemble *"cis"*-SNARE complexes. To block SNARE disassembly, we took advantage of a previously

described mutant of α-SNAP that binds to the SNARE complexes but fails to activate NSF (Barnard et al., 1997).

3.3.1. Recombinant α-SNAP blocks exocytosis which can be restored with NSF or cytosol for wild-type form of the protein but not for the dominant negative (L294A) variant.

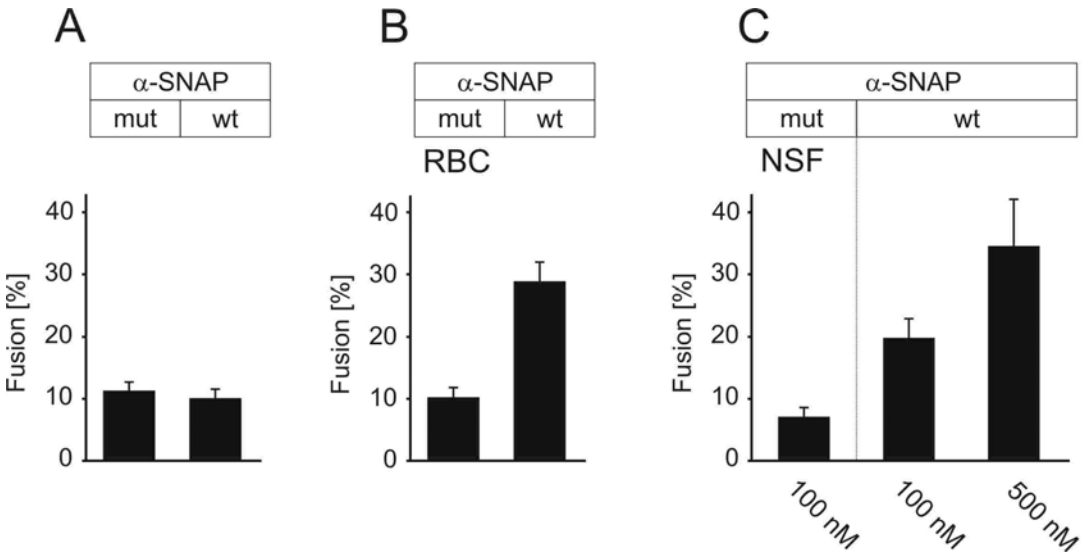

***Figure 16* – (A) Dominant negative effect of α-SNAP (L294A) was observed after its application in the cell-free assay for exocytosis. Similar inhibitory effect was induced by wild-type α-SNAP, which, however, could be ameliorated by co-treatment with rat brain cytosol extracts (RBC) (B), or recombinant *N*-ethylmaleimide sensitive factor (NSF), (C).**

(**A**) Membrane lawns were generated as described and preincubated in K-Glu-DPTA buffer for 5 min with 2 μM wild-type or α-SNAP (L294A). (**B**) Lawns were treated with cytosol (RBC) in presence of either variant of α-SNAP. (**C**) Membranes were incubated with NSF in conjunction with wild-type or α-SNAP (L294A). In all instances, membranes were triggered with K-Glu-

DPTA/Ca^{2+} buffer as described. In a negative control experiment buffer used for the triggering was K-Glu-DPTA. All values are mean ± SEM. n = 8 – 18 membrane lawns per condition.

The dominant negative form of α-SNAP known to be defective in stimulating ATP-dependent activity of NSF was included in preincubation buffer at concentration of 2 μM. It inhibited fusion as reported previously (Barnard et al., 1997) and reduced fusion of secretory granules on membrane lawns from positive control level of 30,1 % ± 3,3 (see **Fig. 17 A**) to 11,3 % ± 1,4 (**Fig. 16 A**). This inhibition could not be relieved by co-incubation of α-SNAP (L294A) with rat brain cytosol (RBC) or *N*-ethylmaleimide sensitive factor (NSF) which would still be bound onto membranes or provided exogenously (**Fig. 16 B** and **C**). To ensure that the effect of the α-SNAP (L294A) is indeed due to a prevention of SNARE disassembly, parallel experiments were performed with the wild-type of α-SNAP. Surprisingly, wild-type form of α-SNAP was as potent as α-SNAP (L294A) in inhibiting exocytosis (**Fig. 16 A**) resulting in a decrease of exocytotic activity to negative control levels - 10,0 % ± 1,4, however, this effect could be alleviated for wild-type α-SNAP by its co-incubation with NSF. Rescue with NSF seemed to be dose-depended as application of 500 nM NSF had more profound rescue effect than 100 nM, which restored exocytotic activity, however, not to its full extent (**Fig. 16 C**). No such rescue effect was observed for α-SNAP (L294A). Similar rescue was possible after co-incubation of wild-type α-SNAP with 0,5 mg/ml rat brain cytosol (RBC) which relieved block of exocytosis only for the wild-type variant of α-SNAP.

Together these findings are difficult to reconcile with the view that the effect of α-SNAP is caused by blocking NSF-disassembly of cis-complexes. Wild-type α-SNAP does not interact with NSF unless bound to SNARE complexes (Whiteheart et al., 1992), and thus an excess of α-SNAP would not interfere with NSF action on SNARE complexes.

3.3.2. Inhibition of NSF by NEM does not inhibit exocytosis in an *in vitro* assay.

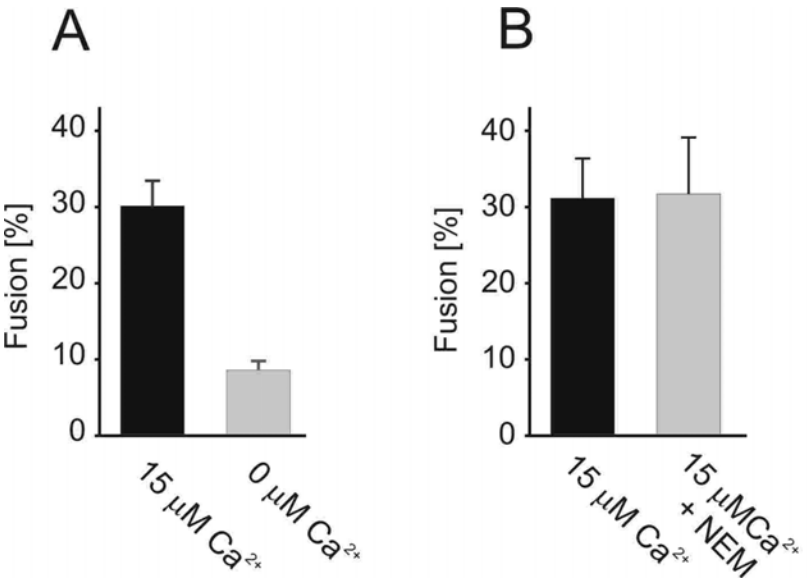

Figure 17 **– Fusion of secretory granules is not affected by NEM in a cell-free assay for exocytosis.**

(**A**) Results of control experiments depicting exocytotic activities after standard treatment of lawns as described in **Methods** section. (**B**) NEM at concentrations ranging from 500 nM to 1 mM (the latter shown in the figure) was included in the K-Glu-DPTA, i.e. the preincubation buffer. All values are mean ± SEM. n = 6 – 18 membrane lawns per condition.

To exclude the possibility that NSF is required for exocytosis in our system, the lawns were preincubated with 1 mM N-ethylmaleimide (NEM). This concentration of NEM is known to inhibit fusion in other cell-free fusion reactions, and purified NSF is completely inactivated at much lower concentrations (see also below). As shown in **Fig. 17 B**, NEM had no effect on Ca^{2+}-dependent exocytosis. Control exocytotic activity did not differ from activity recorded in the presence of NEM and was at the level of 31,1 % ± 5,2 and 31,7 % ± 7,4, respectively.

3.3.3. Biochemical approach to identify a putative effector of α-SNAP binding

The experiments described above document that exocytosis is independent of NSF, ruling out that SNARE-disassembly is required for exocytosis to proceed. However, the data also show that both wild-type and α-SNAP and α-SNAP (L294A) that is impaired in its ability to interact with NSF strongly inhibited fusion. The question then arises how α-SNAP is capable of inhibiting exocytosis, or more precisely, which protein is the target of α-SNAP and by which mechanism α-SNAP-binding to this target blocks fusion. Previous *in vitro* studies involving purified proteins in solution showed that α-SNAP not only binds to fully assembled SNARE complexes but also to uncomplexed syntaxin 1, albeit with lower affinity (McMahon and Sudhof, 1995). A-SNAP was also shown to interact with SNAP-25 but with an at least 10-fold lower affinity whereas no interaction was observed with synaptobrevin (Hanson et al., 1995). These initial findings, which revealed the phenomena presented in two previous sub-chapters, drove my interest towards identification of α-SNAP binding

partner. A likely candidate for such interaction is syntaxin 1 as it has been reported to bind α-SNAP *in vitro* (Hanson et al., 1995). Under experimental conditions, both wild-type and α-SNAP (L294A) would bind to Syx 1 and thereby prevent it from forming fully functional SNARE complexes. This could have impact on membrane fusion measured as the extent of exocytosis in my assay.

To address this question, I performed experiments whose aim was to try to identify by biochemical means whether α-SNAP binds to syntaxin 1 on membrane lawns. Firstly, in order to characterize basic properties of α-SNAP binding to membranes, I tested how fast α-SNAP can bind to membrane lawns and whether this binding interferes in any way with immunoreactivity of syntaxin 1 resident there.

3.3.3.1. Characterisation of α-SNAP and syntaxin 1a immunostaining experiments on membrane lawns

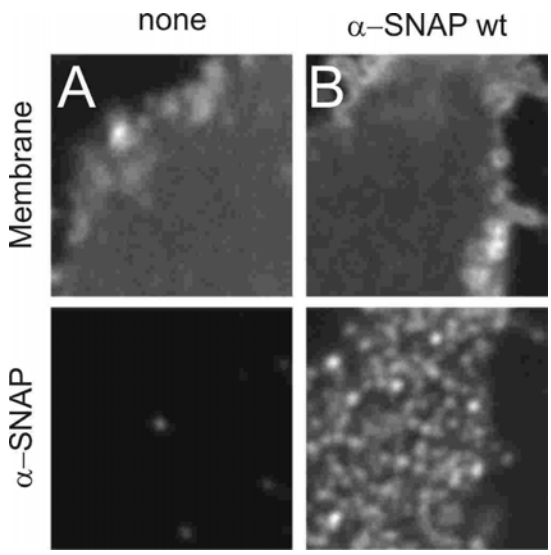

***Figure 18* – (A) Immunostaining of the native α-SNAP on the freshly prepared membrane lawns. (B) Picture of exogenously added α-SNAP that bound and was immunostained on the lawns.**

Membrane lawns were generated as described and were not treated with α-SNAP (**A**) or incubated for 5 min at 37°C with 2 μM wild-type (**B**) or α-SNAP (L294A) (not shown) and then washed with PBS, fixed, and immunolabelled for α-SNAP. Lower panel in (**A**) shows typical staining pattern of a membrane lawn untreated with either variant of α-SNAP indicating that virtually no native α-SNAP was bound to intact membranes. Upper panels show the plasma membranes stained with unspecific lipophillic dye TMA-DPH.

Visualization of a pattern of α-SNAP binding to membranes was preformed with monoclonal antibody (Cl 77.2) which made it possible to label native and both

recombinant α-SNAP forms (wild-type and the L294A) applied and bound onto lawns. When membranes were incubated for 5 min in buffer without α-SNAP and then labelled for any native protein that may have been retained the result showed virtually no α-SNAP bound to lawns (**Fig. 18 A**). To exclude that α-SNAP was washed off during incubation control coverslips were fixed immediately after lawns have been generated. Staining did not differ from one shown in panel (**A**) (data not shown). Wild-type α-SNAP gave a punctate pattern as shown in (**Fig. 18 B)**.

The recombinant α-SNAP binds to the plasma membrane lawns, furthermore, the immunostaining was punctate reminiscent of syntaxin 1 labelling on membranes (Lang et al., 2001).

3.3.3.2. Optimization of α-SNAP binding conditions

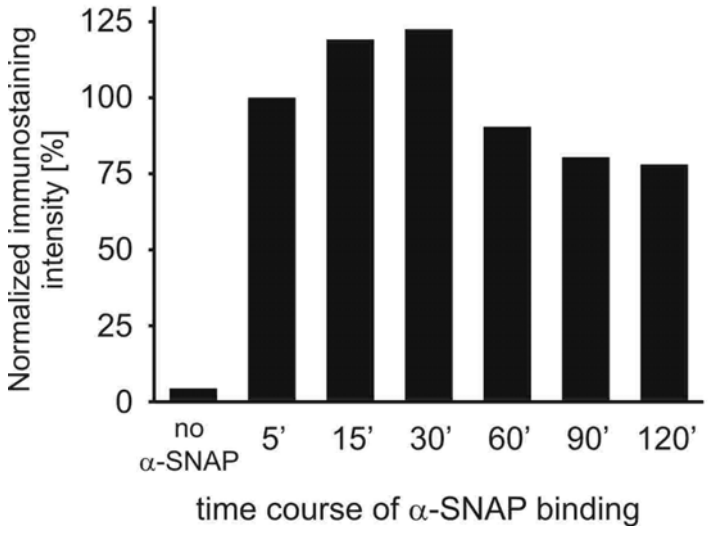

***Figure 19* – Characterization of α-SNAP binding to membranes over time**

◄ Previous page, Cells were sonicated off-stage, i.e. not on microscope as described in **Methods.** Wild-type α-SNAP was added to membrane lawns at 2 μM concentrations and preincubated with them for progressively increasing periods of time. Binding and time course of α-SNAP (L924A) (not shown) was virtually identical to its wild-type form. Experiment was performed twice.

It could be demonstrated that α-SNAP binding to the lawns is quick. Quantification of intensities of immunostaining showed that 5 min preincubation with this protein was enough to approach close-to-saturation binding to the plasma membrane (**Fig. 19**). Extending the incubation did not lead to significantly more pronounced binding to membranes. The fluorescence intensity value obtained after 5 min preincubation with α-SNAP served as 100 % reference value to which all other values presented in this figure were normalized.

Next question addressed concerned capacity of rat brain cytosol and NSF in removal of α-SNAP bound to the freshly prepared membranes. In order to correlate the observed inhibition of exocytosis (see **Fig. 16**) with the membrane-associated binding partner of α-SNAP series of experiments presented below was conducted.

3.3.3.3. A-SNAP is removed from membranes by an active component of rat brain cytosol.

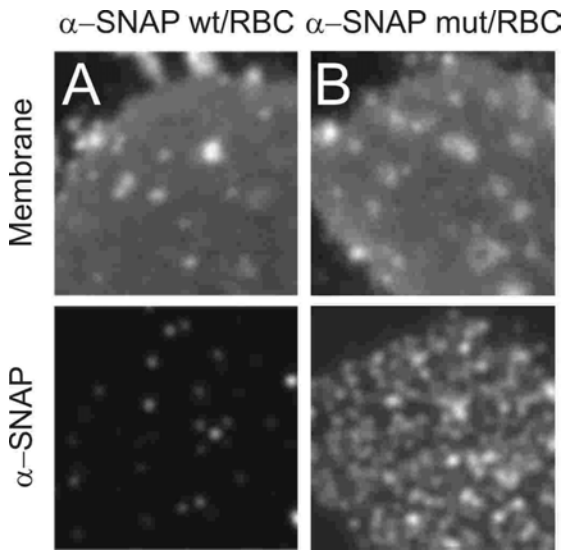

Figure 20 **– Removal of wild-type α-SNAP but not α-SNAP (L294A) bound onto membrane lawns**

Membrane lawns were generated as described and were treated with 2 μM wild-type α-SNAP or α-SNAP (L294A) and then washed with PBS, fixed, and immunolabelled. Pictures show staining patterns after co-incubation of wild-type **(A)** and α-SNAP (L294A) **(B)** with rat brain cytosol. As in **Fig. 18**, the upper panels show the plasma membranes stained with unspecific lipophillic dye TMA-DPH.

The co-incubation of α-SNAP with RBC caused pronounced reduction in staining intensity (**Fig. 20 A**) that closely resembled picture of native α-SNAP (see **Fig. 18 A**). The mutant variant of α-SNAP could bind with the same affinity to membrane lawns (data not shown) although it was not removed from it with RBC (**Fig. 20 B**).

The same set of experiments was done with the recombinant purified NSF and yielded virtually the same result – removal of the wild-type α-SNAP and retention on membranes of the α-SNAP (L294A) variant (data not shown). These data sets demonstrate that α-SNAP is able to bind to freshly prepared fragments of the plasma membrane and this binding can be very strongly reduced with cytosolic extracts of rat brain but only for the wild-type form of α-SNAP and not for the L294A variant.

It could be shown that α-SNAP is able to bind to freshly prepared membrane fragments and this binding can be very strongly reduced with cytosolic extracts of rat brain. This observation combined with results of cell-free assay outcome (see: **Sub-chapter 3.3.1.)** might indicate that membrane-resident SNARE proteins are capable of binding α-SNAP with high affinity. The binding of α-SNAP exhibits the same properties as the inhibition by α-SNAP of exocytosis, strongly suggesting that the binding site observed by immunocytochemistry is identical to the receptor that is responsible for the block in exocytosis.

To further characterize and to quantify the extent of the effects observed on membranes, analyses of several conditions were performed and are presented in the next figure.

3.3.3.4. Incubation of lawns with NSF and rat brain cytosol extracts reduces α-SNAP immunoreactivity indicating possible removal of protein from membrane surface.

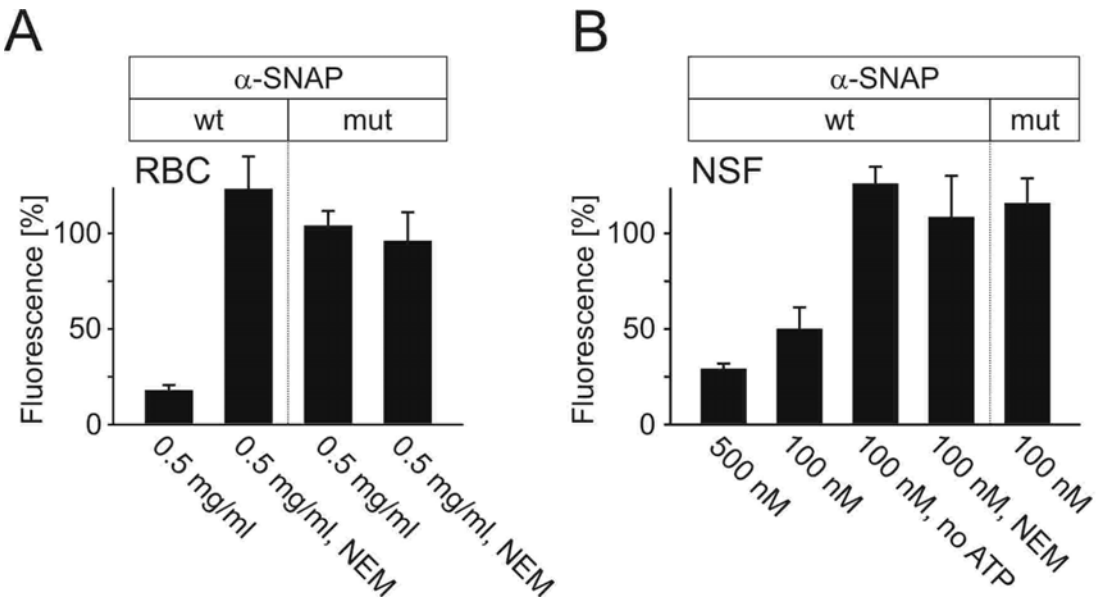

Figure 21 – **Quantification of removal of wild-type and α-SNAP (L294A) with NSF and RBC from membrane lawns.**

Membranes were generated and treated as in the previous experiment. Preincubation buffer contained wild-type or α-SNAP (L294A) together with rat brain cytosol which was or was not treated with 1mM NEM (**A**), or it contained NSF at concentrations of 500 and 100 nM. In some experimental conditions NSF was inactivated by NEM or by the lack of ATP in preincubation buffer (**B**). For respective α-SNAP variant, its fluorescence was normalized with values shown in the **Figure 24 A** set as 100 %.

Membrane lawns were incubated with wild-type α-SNAP or α-SNAP (L294A) and rat brain cytosol (RBC) which for part of experiment was inactivated with NEM. Rat brain cytosol removed wild-type α-SNAP off membranes as observed previously.

Inactivation of RBC with NEM resulted in retention of protein on membranes. No removal was observed when α-SNAP (L294A) was used with combination with RBC or NEM-treated RBC (**Fig. 21 A**). To test, whether application of NSF would mimic the removal effect of RBC, membranes were incubated with two concentrations of NSF – 100 and 500 nM. At both concentrations NSF was capable of removing wild-type α-SNAP and this effect was seemingly larger for the higher concentration of NSF. Surprisingly, 500 nM recombinant NSF was not as efficient as RBC at the concentration of 0,5 mg/ml. When NSF was inactivated by NEM, or when the incubation buffer did not contain ATP required for stimulating NSF action no wild-type α-SNAP was removed from membranes. Based on these and previous findings, α-SNAP (L294A) was not expected to be removed by NSF and this was confirmed experimentally (**Fig. 21 B**)

Three independent approaches were used to examine whether the α-SNAP binding site on the membrane sheets is identical with one of the SNARE proteins – syntaxin 1. First, I performed a competition experiment where I addressed the question of syntaxin 1a being binding partner of α-SNAP. Secondly, I did double labelling experiments to examine whether α-SNAP and syntaxin 1 are co-localized. Third approach took advantage of various clostridial neurotoxins removing enzymatically specific SNARE proteins, among them syntaxin 1 cleaved by BoNT C1.

3.3.3.5. Increasing concentrations of α-SNAP reduce the immunoreactivity of syntaxin 1a resident in the plasma membrane lawns.

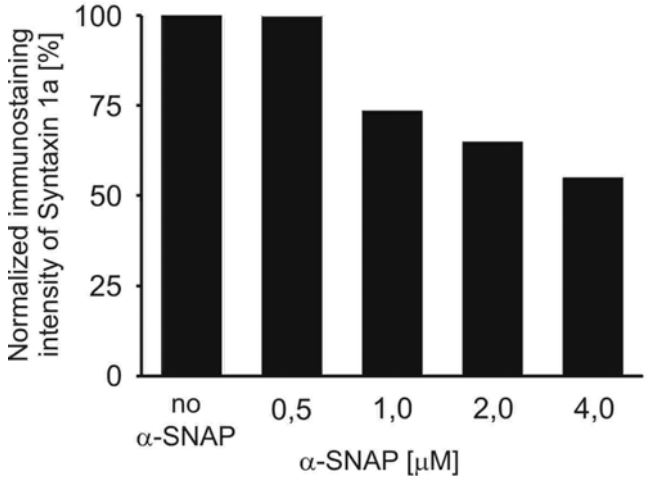

Figure 22 – **Decrease in immunoreactivity of syntaxin 1a after application of increasing concentrations α-SNAP**

Cells were sonicated off-stage, i.e. not on microscope as described in **Methods.** A-SNAP was incubated for 5 min and concentration was varied from 0.5 to 4.0 μM. After the preincubation period, membranes were washed with PBS, fixed and immunolabelled for syntaxin 1a as described. First bar on graph represents fluorescence value to which all other values were normalized to. Experiment was performed twice.

In this experiment, I tested whether increasing amounts of α-SNAP would bind to its target, possibly syntaxin 1, exposed on membranes. The decrease of syntaxin 1a immunoreactivity seemed to correlate with increasing concentrations of α-SNAP and although this effect was not very large, the dose-dependent effect could be observed

(**Fig. 22**). First bar on this graph represents membrane lawns which were not treated with α-SNAP and were immunolabelled with anti-Syx 1a antibody. All other values on this graph were normalized to this reference value.

3.3.3.6. Double immunolabelling on membranes shows high degree of co-localization between syntaxin 1a and α-SNAP bound there.

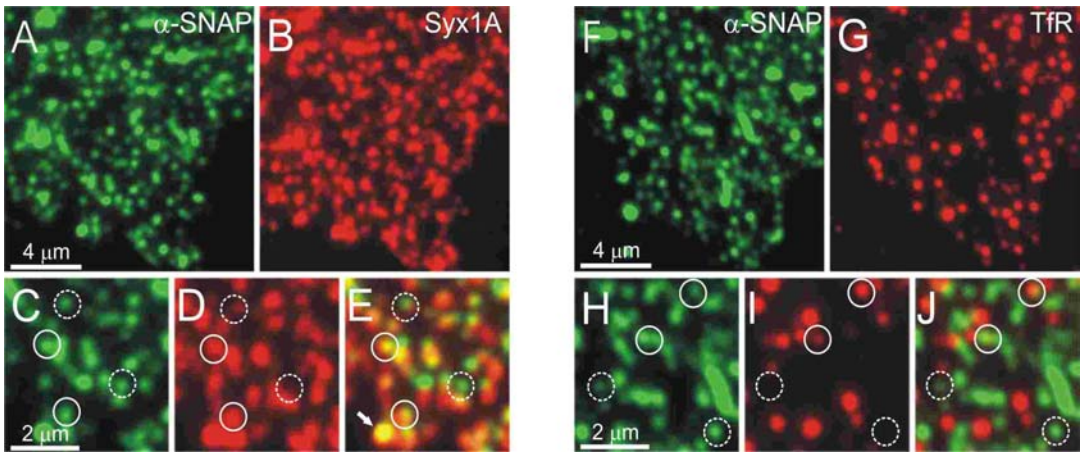

Figure 23 **– Co-localization of α-SNAP with syntaxin 1a but not transferrin receptor on membrane lawns.**

Double-immunolabelled membranes were stained with antibodies against both α-SNAP and syntaxin 1a (**A-E**), or against α-SNAP and transferrin receptor (TfR) **(F-J).** Both panels show an overview of the labelled membranes with magnified areas where co-localization was inspected. Images were analyzed with MetaMorph to quantify the extent of co-localization between a probable binding partner of α-SNAP – syntaxin 1a. Experiment with TfR served as a negative control since no co-localization was expected to take place between these two molecules.

Comparison of representative images revealed a high degree of overlap (**Fig. 23 A – E**). Quantitative analysis revealed that at least 58 % of all α-SNAP positive puncta co-localize with syntaxin 1. As control, double labelling was performed for the transferrin receptor (**F – J**), a single-pass integral membrane protein that cycles between endosomes and the plasma membrane. The transferrin receptor also yielded a punctate staining pattern although less dense than that of syntaxin 1. The degree of overlap was determined to be 9%.

3.3.3.7. Incubation of lawns with clostridial botulinum toxin C1 caused strong reduction in immunoreactivity of α-SNAP.

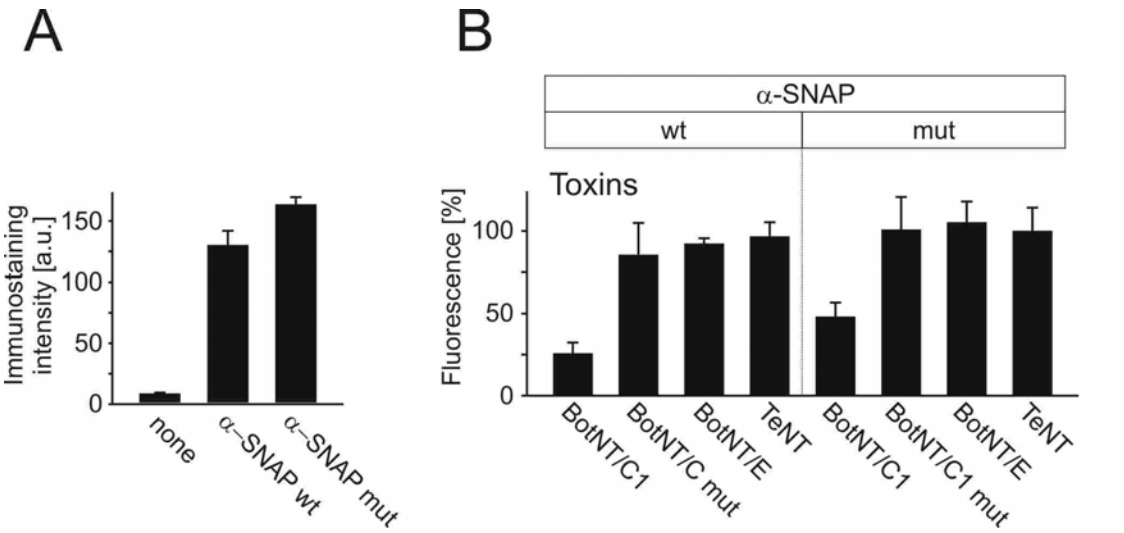

***Figure 24* – (A) Quantification of intensities of immunoreactive wild-type and α-SNAP (L294A) on membranes. (B) Removal of Syx1 by BoNT C1 leads to loss of α-SNAP reactivity.**

Panel (**A**) shows staining intensity (background corrected) of native α-SNAP bound to membranes or of both exogenously provided α-SNAP variants. All

values shown in (**B**) and in **Figure 21** were normalized for fluorescence of respective α-SNAP variant shown in (**A**) that was set as 100 %.
(**B**) Immunolabelled membranes were prepared and treated with various clostridial toxins at concentrations of 2 μM as described and analyzed with to quantify the BoNT C1-dependent removal of α-SNAP from lawns' surface.

I analysed binding of α-SNAP in the presence of recombinant light chain of botulinum neurotoxin C1 (BoNT C1) that selectively cleaves uncomplexed and membrane-bound syntaxin 1. Despite the relatively short incubation time of 5 min, binding was dramatically reduced for both wild-type and mutant α-SNAP (**Fig. 24 B**). No inhibition was observed when a catalytically inactive mutant of the toxin light chain was used. Similarly, neither tetanus toxin (that cleaves synaptobrevin 2) nor botulinum neurotoxin E (that cleaves SNAP-25) had any effect on α-SNAP binding. Together these data show that syntaxin 1 is the main binding site for α-SNAP on the membrane sheets. This idea is additionally supported by data from the previous double immunostaining experiment.

The results of experiments with neurotoxins' light chains demonstrate that indeed the binding partner of α-SNAP on membranes is syntaxin 1. These findings corroborate the hypothesis that α-SNAP inhibits stimulated exocytosis in a cell-free system by binding to free syntaxin 1 possibly preventing it from full assembly required for Ca^{2+}-triggered fusion.

4. Discussion

In this thesis, the characterisation and results obtained with an improved cell-free assay for exocytosis in PC12 cells are described.

The assay presented here is a further improvement over an already existing system developed in the laboratory of Reinhard Jahn. In the new assay developed during my PhD studies in this laboratory, neuroendocrine PC12 cells grown on glass coverslips were disrupted ultrasonically on the microscope stage. Resulting membrane lawns were preincubated for 5 min with various soluble factors (e.g. ATP-Mg, soluble SNAREs, α-SNAP) and triggered with Ca^{2+} to initiate the exocytotic fusion of content-labelled secretory granules. The entire process was monitored by fluorescence microscopy at the single granule level.

Reduction of the delay between the loss of cell integrity and the measurement of exocytosis is the major feature of this assay and is in contrast to the previously used systems. By applying the time window typically encountered in whole-cell patch clamping it is possible to access and probe the late steps in the exocytotic pathway. This was not possible previously when the long time-delay resulted in the biochemical run-down and loss of activated states in the preparation.

4.1. Establishment of the improved cell-free assay for exocytosis

Freshly prepared lawns closely resemble intact plasma membranes and offer a possibility for testing of a broad array range of factors influencing exocytosis. In my

system, secretory vesicles are left docked on the plasma membrane at the beginning of the experiment, whereas cytosol and all organelles are removed. Ca^{2+}-dependent exocytosis in this system does not require soluble cytosolic factors, and it does not require disassembly of SNAREs as a priming step, setting it apart from all other cell-free assays for membrane fusion.

The use of such an approach in these studies allows for tackling the problem of what are the minimal essential components required for efficient priming and subsequent fusion. I could address the question how the processes leading to exocytosis are modulated upon addition of different SNARE-interacting proteins or other non-proteinaceous factors that are known to play a role in the heterotypic fusion of membranes. For this purpose, it was instrumental to introduce a 5 min preincubation time period to allow these compounds to exert their action on membranes. The exocytotic activity measured afterwards was not different from the observed on lawns triggered immediately without the preceding preincubation yielding an appropriate time window for differentiating events occurring before and after triggering with Ca^{2+}.

4.2. Characterisation of the exocytotic responses in the improved cell-free assay

Dependence of exocytosis on ATP-Mg has been postulated previously (Hay and Martin, 1992) but the problems with access to the interior of permeabilized PC12 cells assay did not allow for clear separation between cytosol- and ATP-Mg-dependent steps. Cracked neuroendocrine cells are limited in the possibility of re-supplying proteins and metabolites washed out during permeabilization. In my assay it is possible to test the effects of various factors including small molecules like ATP-Mg or its analogues and of proteins. Previous studies in permeabilized chromaffin cells revealed that a much larger number of LDCVs undergo calcium-activated exocytosis in the presence of ATP-Mg than in its absence (Parsons et al., 1995). This number exceeded the number of morphologically docked vesicles, indicating that ATP-Mg was also required for the recruitment of vesicles to the plasma membrane.

In PC12 cells, secretion from a cellular fraction containing secretory granules tightly associated with plasma membrane fragments was strictly dependent on calcium and ATP-Mg (Martin et al., 1995; Martin and Kowalchyk, 1997). However, little is known about the exact order and requirements of these energy-dependent steps.

To address the question of cytosol and ATP-Mg-dependences, I performed series of experiments in which these two factors were thoroughly tested.

4.2.1. Exocytosis in cell-free assay is dependent on the continuous presence of ATP.

Processes of membrane fusion depend on energy supply provided by ATP-Mg. Several studies performed in neuroendocrine PC12 and chromaffin cells showed such partial dependence of some stages in the exocytotic pathway (Hay and Martin, 1992; Holz et al., 1989).

In my assay, ATP-Mg had to be present during both, the preincubation and the triggering phase to maintain exocytosis. Removal of ATP-Mg from the preincubation or the triggering phase reduced fusion. The extent of this reduction was dependent on the experimental stage, which ATP-Mg was absent from. Loss of activity seen when ATP-Mg was absent from the preincubation phase could be ascribed to an irreversible depriming of the previously primed and fusion-competent granules. This suggests that the ATP-dependent reactions are required downstream of SNARE disassembly. Such depriming, i.e. rundown of some crucial ATP-Mg-dependent mechanisms that are responsible for maintenance of fusion readiness, has been reported in semi-intact PC12 cells (Hay and Martin, 1992) and chromaffin cells (Holz et al., 1989). When primed cells were incubated without ATP-Mg, their capacity for rapid Ca^{2+}-dependent exocytosis was readily lost. Interestingly, in these experimental systems, ATP-Mg seemed to have no or very little effect on exocytosis after the priming was completed. In contrast to this finding, secretion in my assay displayed certain degree of ATP-Mg-dependence during the triggering phase.

A possible explanation of this observation is requirement of ATP-Mg for the completion of an ongoing priming of non-fully primed secretory granules. If a subpopulation of un-primed or deprimed granules is present on membranes, then it is possible that the lack of ATP-Mg during the triggering phase prevents these granules from the completion of priming and subsequent exocytosis. If, however, ATP-Mg is provided throughout the course of experiment, perhaps the un-primed and/or deprimed granules are capable to achieve fusion-competent state and release their content upon arrival of the Ca^{2+}-trigger.

4.2.2. Various ATP analogues inhibit exocytosis when introduced in the cell-free assay.

Non-hydrolysable analogues of ATP were previously applied to probe ATP-dependence of exocytosis in many various assays for exocytosis (Baker and Whitaker, 1978; Whalley et al., 1991). Reagents like AMP-PNP cannot be hydrolyzed by ATPases or by kinases inducing thereby massive inhibition of most, if not all, ATP-requiring steps. To avoid such global action exerted by these compounds, another analogue - ATPγS has been tested in assays for exocytosis. It can be hydrolyzed by some kinases but not by ATPases. Results of capacitance and amperometric patch-clamp measurements revealed that it inhibited the exocytotic burst and the slow phase of release (Xu et al., 1998). Interestingly, in one study performed in PC12 cells, it was shown that ATPγS exerted stimulatory effect (Vu and Wagner, 1993).

In my assay, both analogues were capable of inhibiting exocytosis. Most potent inhibition was observed when one or the other analogue was present during the triggering phase. This effect must have been very rapid because the delay between the wash-out of the ATP-Mg-containing priming buffer and application of the Ca^{2+}-containing triggering buffer supplemented with either analogue is in the range of seconds. This would indicate that both analogues caused almost instantaneous depriming of all fusion-competent granules rendering them incapable of fusion.

The effects caused by the analogues were not identical with simple omission of ATP-Mg from the triggering stage. In case of sheer ATP-Mg-omission, the exocytosis was reduced, albeit not as dramatically as observed after the application of either analogue.

The observation that the introduction of an analogue is not identical with ATP-Mg omission was supported with results of the experiments with one or the other analogue present during the preincubation. Inclusion of an analogue in this phase did not lead to an irreversible depriming but rather prevented it, since the following triggering of fusion with the ATP-Mg-containing buffer yielded considerable exocytotic activity.

These observations are somewhat difficult to explain in the light of the earlier findings (Xu et al., 1998), as it has been reported that ATPγS and AMP-PNP can completely block fusion in PC12 and chromaffin cells after 5 min-long perfusion. It is possible that in my assay these compounds do not work in the same manner as in

semi-intact cells perfused with them. It is also possible that the ATP analogues replace ATP-Mg at its binding sites and thereby protect exocytotic machinery from rapid run-down normally caused by the lack of ATP-Mg as demonstrated in the respective experiments discussed above.

4.2.3. Cytosolic factors are not required for exocytosis but modulate this process in the presence of ATP.

Studies in permeabilized PC12 and chromaffin cells supported the idea that cytosolic components are required for priming of the exocytotic machinery to achieve efficient fusion after arrival of Ca^{2+}-trigger (Hay and Martin, 1992; Holz et al., 1989).
Based on the data obtained in this thesis I conclude however, that rat brain cytosol is not required for maintaining a primed state and that the key factor for this process is ATP.

As discussed above, the lack of ATP-Mg during the preincubation stage led to an irreversible depriming, despite subsequent presence of ATP-Mg during the triggering phase. However, presence of cytosol seemed to prevent such loss of activity possibly due to the combined action of, yet unidentified, cytosolic protein or proteins. Such prevention (or "re-priming") of a deprimed state (or activity run-down) was not complete, however.
In another series of tests cytosol was present throughout the course of experiment whereas ATP-Mg was introduced only in the preincubation or the triggering stage.

In the latter case, action of cytosol prolonged past the preincubation stage might make it inhibitory and thereby causing reduction in exocytosis. Under these circumstances, gradual depletion of ATP-Mg from the preincubation buffer by cytosol could cause the observed decrease of the exocytotic activity.

Taken together the data from these sets of experiments, it seems that the ATP-Mg-dependent re-priming requires the presence of cytosol. The exact nature of such reactivation remains unknown. Lack of this assay's dependence on cytosol makes it different from noradrenaline release in permeabilized PC12 cells, which is abolished upon omission of cytosol (Hay and Martin, 1992).

4.2.4. SNARE-specific neurotoxins strongly reduce fusion on membrane lawns however do not abolish it.

Susceptibility of SNARE proteins to the action of specific metalloproteases was used as a means for probing nearly-native SNAREs exposed on the inner side of the plasma membrane. Most of the toxins light chains applied were able to reduce the exocytotic activity in my assay by 50 – 60 %.

The fact that BoNT C1 and D exhibited strongest effects can be linked to their molecular targets – syntaxin 1 and synaptobrevin 2. Enzymatic cleavage with BoNT C1 led to the removal of syntaxin 1 and in consequence, to efficient incapacitation of one the fusogenic SNAREs. An effect of the same severity was observed after cleavage of the R-SNARE – synaptobrevin 2 with BoNT D. Although, removal of either Syx 1 or Syb 2 was expected to lead to a complete block of fusion as assumed

from *in vitro* data (Yamasaki et al., 1994) or semi *in vivo* recordings (Chen et al., 2001), this was not observed in my assay to the same extent.

Incomplete inhibition of fusion is in line with previous some studies of regulated and constitutive secretion, in which such a blockade of release was rarely complete (Capogna et al., 1997; Lawrence et al., 1994). One possible explanation of this phenomenon is a relatively short time of preincubation (5 min) during which the toxins act. Taken into account that these proteins do not instantaneously cleave off all their SNARE targets, it is possible to ascribe an incomplete inhibition to the slow rate of SNARE incapacitation. Another explanation of this effect is a possibility of bypassing this inhibition suggesting that parts of machinery responsible for driving fusion are protected from proteolytic activity of the toxin light chains.

It cannot be excluded that in the moment of cell rupture, a large population of SNARE proteins is already complexed into tight *"trans"*-SNARE complexes and thus inaccessible to respective toxins. When lawn is generated any vesicle cycling is halted and the pre-existing SNARE complexes are caught at various stages of assembly, including *"trans"*-complexes. It is conceivable, that the fraction of these complexes is resistant to toxins (Hayashi et al., 1994; Hayashi et al., 1995; Ryan, 1998). This would be in contrary to *in vivo* situation when SNAREs on vesicles cycle uninterrupted during incubation with toxin cleaving gradually most uncomplexed SNAREs. Experiments done on crayfish neuromuscular junction support this view, as nerve stimulation increased the TetNT-dependent build-up of blockade of neurotransmitter release (Hua and Charlton, 1999). Because SNAREs need to undergo disassembly leading to their toxin-sensitive monomerization, this likely

causes the incapacitation of most of them during this process what cannot be observed to the same degree in my assay.

A possible mechanism to explain observed reduction in the exocytotic activity caused by BoNT A is based on the site of cleavage of this toxin. It removes off SNAP-25 the last nine amino acids at the C-terminal end leaving the molecule truncated but still able to form SNARE complexes that could drive fusion (Xu et al., 1998) and that can be disassembled by NSF (Otto et al., 1995). Virtually the same experimental outcome as observed after treatment with BoNT A – reduction of exocytosis by ~60 %, was observed after application of BoNT E. *In vitro* experiments have shown that this toxin cleaves additional 17 C-terminal amino acids than BoNT A (Binz et al., 1994) what would suggest observing more profound reduction of exocytosis than after application of BoNT A. This treatment, however, did not seem to reduce fusion in my cell-free assay to a greater degree than BoNT A.

Tetanus toxin-induced inhibition of exocytosis was similarly potent but lower than expected since data obtained from chromaffin cells or PC12 cells (De Haro et al., 2003) showed that it was possible to completely abolish fusion with light chain of this protein. On the other hand, this inhibition could be bypassed in rat synaptosomes by maintaining elevated levels of Ca^{2+} by introduction of calcium ionophore (Fassio et al., 1999).

These results show that all light chains of clostridial neurotoxins were able to strongly reduce exocytosis in the cell-free assay described. These effects can be ascribed to partial invulnerability to toxins' light chains that some of "trans"-complexes incorporating SNAREs would exhibit.

4.2.5. Soluble domains of SNARE proteins and SNARE-specific antibodies inhibit exocytosis.

To further characterize my cell-free assay I decided to take advantage of an additional set of molecular tools used previously to address questions of SNARE availability. Addition of peptides corresponding to the SNARE motifs or application of antibodies against them showed that the native SNAREs can be efficiently incapacitated as demonstrated by studies in permeabilized PC12 (Hua and Scheller, 2001) or chromaffin cells (Xu *et al.,* 1999).

Similarly to the experiments involving neurotoxins, the soluble domains of SNARE proteins tested in my assay strongly inhibited fusion on membrane lawns. Regardless of the stage at which given soluble SNARE was administered or the type of SNARE protein, they could reduce exocytosis by 50 – 60 %. Application of two Q-SNAREs: SNAP-25 and syntaxin 1a throughout the course of the entire experiment caused virtually complete inhibition of exocytosis. This block could be explained by binding of both proteins to the uncomplexed synaptobrevin 2 on the surface of secretory granules. Such binding would lead to formation of inactive *"cis"*-SNARE complexes of granules what in turn would arrest them from fusing with the plasma membrane. It is unclear, whether such inhibition would be exerted by a direct binding of SNAP-25 and Syx 1a to synaptobrevin 2, or it involves prior formation of SNAP-25/Syx 1a complex as demonstrated in an *in vitro* system (Fasshauer, 2003). It cannot be excluded that SNARE complexes on the remaining active 40 % of secretory granules were present in a tight *"trans"* form. This would prevent soluble domains of SNARE

proteins from binding to their native counterparts and from even more profound inhibition.

The reduction of exocytosis after application of Syb 2 can be also explained by the formation of an inactive *"cis"*-SNARE complex. Slightly lesser efficiency of inhibition after application of synaptobrevin 2 might reflect reduced accessibility of this protein to the helices of SNAP-25 and syntaxin 1 in comparison to SNAP-25/Syx 1-induced block.

It is possible that a large fraction of native SNARE proteins associated with secretory granules on membrane lawns can be accessed by externally provided SNAREs. Docked but not yet fully primed granules would be susceptible to block caused by soluble SNAREs as some of their complexes were not fully zippered. The remaining population of SNARE proteins would be assembled in tight *"trans"*-complexes that could not be blocked by the exogenous domains of SNAREs.

In addition to use of soluble SNAREs, several antibodies against SNAREs have been applied to probe the status of these molecules. Findings in the chromaffin cells showed that slow phases of exocytosis can be inhibited by the anti-SNAP-25 antibody (Xu et al., 1998).

In my assay this antibody did not reduce exocytosis after 5 min treatment. It might have been caused by inability of Cl 71.1 to access SNAP-25 already complexed into *"trans"*-SNARE complexes mentioned above. Extending the preincubation with Cl 71.1 to 10 min resulted in a strong reduction of the exocytotic activity. It is possible

that the fully assembled and thus partially toxin- and antibody-resistant SNARE complexes undergo disassembly during this 10 min of incubation. This reaction could be due to the biochemical run-down and loss of ATP-activated status by the secretory granules. According to the model of SNARE availability (Xu et al., 1999) such process of "depriming" would be then responsible for liberation of SNAREs from complexes creating thereby access sites for antibody and toxins.

4.3. Function of α-SNAP in exocytotic responses in the *in vitro* assay

In the present study, I have used an advanced cell-free assay for regulated exocytosis to uncover a novel feature of α-SNAP in the SNARE-dependent membrane fusion. Here I show that α-SNAP is capable of directly and potently inhibiting exocytosis unless counteracted by NSF. Moreover, I show that α-SNAP exerts its action by binding to syntaxin 1, preventing it from interacting with its SNARE partners mediating fusion.

4.3.1. Recombinant α-SNAP blocks exocytosis which can be restored for wild-type form of the protein but not for its dominant negative variant (L294A).

The dominant negative form of α-SNAP (L294A) is known to be defective in stimulating ATP-dependent activity of NSF (Barnard et al., 1997). It has been proposed that SNAREs in the plasma membrane are free and most likely under the experimental circumstances they are not rate-limiting factors (Lang et al., 2002). They could be maintained free however, by a possibly existent, membrane-associated

pool of native α-SNAP and NSF. It was not likely, as shown in a part of **Results** and discussed above, because my system was not dependent on cytosol and insensitive to NEM.

Inhibition of fusion my assay by wild-type form of α-SNAP was novel since introduction of α-SNAP generally stimulates intracellular fusion reactions including exocytosis in PC12 and chromaffin cells (Kibble et al., 1996; Xu et al., 1999; Banerjee et al., 1996b). Similar inhibitory effect could be observed only in one instance, namely vacuolar fusion in yeast where addition of yeast homologue of α-SNAP, Sec17p has been reported to inhibit fusion by interference with early pre-docking step (Wang et al., 2000)

The inhibitory effect of wild-type α-SNAP could be alleviated for by its co-incubation with NSF or cytosol in my assay. These results showed that the freshly prepared membrane lawns have the capacity to bind both variants of α-SNAP, which upon this binding blocks exocytotic machinery. The difference in responsiveness of these two variants of α-SNAP suggests an interaction with NSF that is present in cytosol and that differentiates between two α-SNAP species. A-SNAP binding to SNAREs could be responsible for initiation of such block of exocytosis perhaps due to incapacitation of one of the SNARE proteins resident in the plasma membrane.

4.3.2. Incubation of lawns with NSF and rat brain cytosol extracts reduces wild-type α-SNAP immunoreactivity indicating possible removal of protein from membrane surface.

I have been able to show that α-SNAP is capable of binding to freshly prepared membrane fragments and this binding can be reduced with rat brain cytosol. These effects were studied in a systematic manner during the subsequent experiments.

Firstly, I analyzed morphology of α-SNAP staining pattern. It showed that binding of recombinant α-SNAP resulted in strong punctate staining on membranes for both the wild-type and the L294A form. The label of wild-type α-SNAP but not of L294A variant was removed from the lawns by cytosol. In the presence of NEM that inactivates recombinant NSF or NSF present in cytosol, the wild-type form was also retained on the lawns. Furthermore, pre-bound α-SNAP was removed when NSF was added at a later time point indicating that NSF is capable of dissociating α-SNAP from its binding sites on the plasma membrane lawns.

Such removal in case of wild-type α-SNAP and lack of it in case of α-SNAP (L294A) correlates well with the observations made with *in vitro* assay for exocytosis where a rescue of activity correlated with presence of wild-type α-SNAP and RBC during the 5 min-long preincubation phase. This means, that a specific factor present in rat brain cytosol acts only on wild-type α-SNAP causing its dissociation from membrane. The same factor is unable to perform the same task for mutant variant of α-SNAP.

These observations might indicate that membrane-residing SNARE proteins are capable of binding α-SNAP with high affinity. Moreover, my data demonstrate that binding of α-SNAP correlates with the inhibition of *in vitro* exocytosis by α-SNAP. Such correlation strongly suggests that the binding site observed by immunocytochemistry is identical with the receptor that is responsible for the block in exocytosis observed previously.

4.3.3. Biochemical approaches towards identification of a putative effector of α-SNAP binding

Reduction in syntaxin immunoreactivity, as probed with specific antibodies, was observed after binding of α-SNAP to membranes. This initial characterization suggested that the protein involved in binding might be syntaxin 1. It was likely that by its binding to Syx 1, α-SNAP occluded site recognized by a specific anti-Syx 1a antibody thereby reducing syntaxin's immunoreactivity. In other experiments I could show that the binding of α-SNAP is quick and does not strongly increase with prolonged incubation. This was indicated by saturation of membrane binding sites with α-SNAP.

If indeed syntaxin 1 was the target of α-SNAP, then experiments involving enzymatic or cytosol-induced removal of Syx 1 with would give insights about the nature of this binding partner.

4.3.3.1. Double immunolabelling on membranes shows high degree of co-localization between syntaxin 1a and α-SNAP bound there.

In order to precisely identify the binding site I localized α-SNAP by immunocytochemistry on the membrane lawns. Initial findings presented above supported the idea that syntaxin 1 is the binding partner for α-SNAP. Quantitative analysis performed on double-stained microscopic images revealed that at least 58 % of co-localization between α-SNAP and syntaxin 1 puncta. High degree of co-localization corroborates the idea that the binding partner of α-SNAP is indeed syntaxin 1 present in the plasma membranes.

4.3.3.2. Incubation of lawns with the light chain of clostridial botulinum toxin C1 caused strong reduction in immunoreactivity of α-SNAP.

From the toxins experiments data it was concluded that the light chain of BoNT C1 reduces α-SNAP binding to the membranes. No inhibition was observed when a catalytically inactive mutant of this toxin was used. Similarly, neither tetanus toxin and botulinum neurotoxin E had any effect on α-SNAP binding. These findings supported by the co-localization study allowed for concluding that syntaxin 1 is the main binding site for α-SNAP on the membrane lawns.

The results show that α-SNAP inhibits stimulated exocytosis in a cell-free system and that this inhibition can be attributed to binding of α-SNAP to free syntaxin 1 in the

membrane lawns. It is possible that α-SNAP binding directly blocks for formation of SNARE complex by blocking the SNARE motifs. Alternatively, α-SNAP binding may exert its effect further upstream, e.g. by interfering with other proteins that are required before *"trans"*-SNARE complex is formed. It cannot be, however, excluded that α-SNAP exerts its action directly on the *"trans"*-SNARE complex, e.g. by preventing its Ca^{2+}-dependent activation or by interfering with assembly of the complex.

Binding of α-SNAP to syntaxin inhibits fusion unless acted upon by NSF uncovers a second site of action of NSF in the pathway leading towards exocytosis. It remains to be established how exactly the inhibitory action of α-SNAP is exerted. Possibly, the presence of α-SNAP prevents syntaxin 1 from interacting with its SNARE partners. This assumption is supported by the observation that α-SNAP binds to all syntaxin clusters in the membrane irrespectively of whether they contain docked vesicles or not. However, it is also possible that α-SNAP in addition binds to the *"trans"*-SNARE complexes and that this inhibition is only becoming apparent after initial zippering has taken place. If NSF activity becomes rate-limiting, however, α-SNAP-mediated inhibition of exocytosis may become dominant and shut down exocytosis even before dissociated SNAREs are used up and *"cis"*-complexes accumulate. Such situations may arise when intracellular ATP-levels drop, or when NSF action is prevented by other mechanisms. For instance, disruption of the NSF-α-SNAP interaction by peptide-inhibition resulted in a rapid block of neurotransmitter release in the squid giant synapse, which was attributed to a post-docking step (DeBello et

al., 1995). It is possible that this effect may be partially caused by α-SNAP binding to syntaxin rather than accumulation of *"cis"*-SNARE complexes. Shut-down of exocytosis by α-SNAP may thus function as a sensor for NSF activity, ensuring that exocytosis only proceeds if the activity level of NSF suffices to regenerate SNARE complexes. Similarly, α-SNAP-mediated inhibition may prevent massive and possibly excytotoxic discharge of secretory organelles when cells are flooded with Ca^{2+} following a drop in ATP-levels, as it may occur during apoptotic or necrotic cell death. It remains to be tested whether α-SNAP is capable of interacting with other syntaxins in a similar manner, thus being capable of shutting down intracellular membrane traffic unless counteracted by NSF.

Summary

I have developed a cell-free assay for exocytosis based on the generation of membrane lawns containing fluorescent, docked secretory granules that are imaged during exocytosis. Ultrasonic disruption of PC12 cells grown on coated coverslips is performed on the microscope stage in a small chamber and results in the generation membrane lawns that can be triggered with Ca^{2+} to exocytose their eGFP content. Reduction of the delay between the loss of cell integrity and the measurement of exocytosis reduces biochemical run-down on membranes. With this assay it is possible to access and probe the late steps in the exocytotic pathway by applying a wide range of various factors onto freshly made lawns that resemble intact membranes.

I addressed the question of cytosol and ATP-Mg-dependence in this assay and could conclude that in agreement with preceding observations on permeabilized cells, ATP-Mg was vitally required to enable the system to respond to Ca^{2+} trigger. However, the system described in this thesis was not dependent on cytosol what made it different from noradrenaline release in permeabilized PC12 cells.

In the following study, I have used the above cell-free assay to uncover a novel feature of α-SNAP in SNARE-dependent membrane fusion. I could show that α-SNAP is capable of directly and potently inhibiting exocytosis unless counteracted by NSF. Moreover, I show that α-SNAP exerts its action by binding to syntaxin, preventing it from interacting with its SNARE partners to mediate fusion.

References

1. Ann, K., J.A. Kowalchyk, K.M. Loyet, and T.F. Martin. 1997. Novel Ca2+-binding protein (CAPS) related to UNC-31 required for Ca2+-activated exocytosis. *J Biol Chem*. 272:19637-40.

2. Aravamudan, B., T. Fergestad, W.S. Davis, C.K. Rodesch, and K. Broadie. 1999. Drosophila UNC-13 is essential for synaptic transmission. *Nat Neurosci*. 2:965-71.

3. Ashery, U., F. Varoqueaux, T. Voets, A. Betz, P. Thakur, H. Koch, E. Neher, N. Brose, and J. Rettig. 2000. Munc13-1 acts as a priming factor for large dense-core vesicles in bovine chromaffin cells. *Embo J*. 19:3586-96.

4. Avery, J., D.J. Ellis, T. Lang, P. Holroyd, D. Riedel, R.M. Henderson, J.M. Edwardson, and R. Jahn. 2000. A cell-free system for regulated exocytosis in PC12 cells. *J Cell Biol*. 148:317-24.

5. Bajohrs, M., C. Rickman, T. Binz, and B. Davletov. 2004. A molecular basis underlying differences in the toxicity of botulinum serotypes A and E. *EMBO Rep*. 5:1090-5.

6. Barg, S., C.S. Olofsson, J. Schriever-Abeln, A. Wendt, S. Gebre-Medhin, E. Renstrom, and P. Rorsman. 2002. Delay between fusion pore opening and peptide release from large dense-core vesicles in neuroendocrine cells. *Neuron*. 33:287-99.

7. Baker, P.F., and M.J. Whitaker. 1978. Influence of ATP and calcium on the cortical reaction in sea urchin eggs. *Nature*. 276:513-5.

8. Banerjee, A., V.A. Barry, B.R. DasGupta, and T.F. Martin. 1996. N-Ethylmaleimide-sensitive factor acts at a prefusion ATP-dependent step in Ca2+-activated exocytosis. *J Biol Chem*. 271:20223-6.

9. Barg, S., C.S. Olofsson, J. Schriever-Abeln, A. Wendt, S. Gebre-Medhin, E. Renstrom, and P. Rorsman. 2002. Delay between fusion pore opening and peptide release from large dense-core vesicles in neuroendocrine cells. *Neuron*. 33:287-99.

10. Barnard, R.J., A. Morgan, and R.D. Burgoyne. 1997. Stimulation of NSF ATPase activity by alpha-SNAP is required for SNARE complex disassembly and exocytosis. *J Cell Biol*. 139:875-83.

11. Becker, K.A., and N.H. Hart. 1999. Reorganization of filamentous actin and myosin-II in zebrafish eggs correlates temporally and spatially with cortical granule exocytosis. *J Cell Sci*. 112 (Pt 1):97-110.

12. Bennett, M.K., N. Calakos, and R.H. Scheller. 1992. Syntaxin: a synaptic protein implicated in docking of synaptic vesicles at presynaptic active zones. *Science*. 257:255-9.

13. Betz, A., I. Telemenakis, K. Hofmann, and N. Brose. 1996. Mammalian Unc-13 homologues as possible regulators of neurotransmitter release. *Biochem Soc Trans*. 24:661-6.

14. Binz, T., J. Blasi, S. Yamasaki, A. Baumeister, E. Link, T.C. Sudhof, R. Jahn, and H. Niemann. 1994. Proteolysis of SNAP-25 by types E and A botulinal neurotoxins. *J Biol Chem*. 269:1617-20.

15. Blasi, J., E.R. Chapman, E. Link, T. Binz, S. Yamasaki, P. De Camilli, T.C. Sudhof, H. Niemann, and R. Jahn. 1993a. Botulinum neurotoxin A selectively cleaves the synaptic protein SNAP-25. *Nature*. 365:160-3.

16. Blasi, J., E.R. Chapman, S. Yamasaki, T. Binz, H. Niemann, and R. Jahn. 1993b. Botulinum neurotoxin C1 blocks neurotransmitter release by means of cleaving HPC-1/syntaxin. *Embo J*. 12:4821-8.

17. Bloch-Shilderman, E., S. Abu-Raya, V. Trembovler, H. Boschwitz, A. Gruzman, M. Linial, and P. Lazarovici. 2002. Pardaxin stimulation of phospholipases A2 and their involvement in exocytosis in PC-12 cells. *J Pharmacol Exp Ther*. 301:953-62.

18. Bock, J.B., H.T. Matern, A.A. Peden, and R.H. Scheller. 2001. A genomic perspective on membrane compartment organization. *Nature*. 409:839-41.

19. Broadie, K., A. Prokop, H.J. Bellen, C.J. O'Kane, K.L. Schulze, and S.T. Sweeney. 1995. Syntaxin and synaptobrevin function downstream of vesicle docking in Drosophila. *Neuron*. 15:663-73.

20. Brose, N., A.G. Petrenko, T.C. Sudhof, and R. Jahn. 1992. Synaptotagmin: a calcium sensor on the synaptic vesicle surface. *Science*. 256:1021-5.

21. Brose, N., C. Rosenmund, and J. Rettig. 2000. Regulation of transmitter release by Unc-13 and its homologues. *Curr Opin Neurobiol*. 10:303-11.

22. Chamberlain, L.H., D. Roth, A. Morgan, and R.D. Burgoyne. 1995. Distinct effects of alpha-SNAP, 14-3-3 proteins, and calmodulin on priming and triggering of regulated exocytosis. *J Cell Biol*. 130:1063-70.

23. Chamberlain, L.H., R.D. Burgoyne, and G.W. Gould. 2001. SNARE proteins are highly enriched in lipid rafts in PC12 cells: implications for the spatial control of exocytosis. *Proc Natl Acad Sci U S A*. 98:5619-24.

24. Capogna, M., R.A. McKinney, V. O'Connor, B.H. Gahwiler, and S.M. Thompson. 1997. Ca2+ or Sr2+ partially rescues synaptic transmission in hippocampal cultures treated with botulinum toxin A and C, but not tetanus toxin. *J Neurosci*. 17:7190-202.

25. Chen, Y.A., S.J. Scales, S.M. Patel, Y.C. Doung, and R.H. Scheller. 1999. SNARE complex formation is triggered by Ca2+ and drives membrane fusion. *Cell*. 97:165-74.

26. Chen, Y.A., S.J. Scales, J.R. Jagath, and R.H. Scheller. 2001a. A discontinuous SNAP-25 C-terminal coil supports exocytosis. *J Biol Chem*. 276:28503-8.

27. Clary, D.O., and J.E. Rothman. 1990. Purification of three related peripheral membrane proteins needed for vesicular transport. *J Biol Chem*. 265:10109-17.

28. DeBello, W.M., V. O'Connor, T. Dresbach, S.W. Whiteheart, S.S. Wang, F.E. Schweizer, H. Betz, J.E. Rothman, and G.J. Augustine. 1995. SNAP-mediated protein-protein interactions essential for neurotransmitter release. *Nature*. 373:626-30.

29. De Haro, L., S. Quetglas, C. Iborra, C. Leveque, and M. Seagar. 2003. Calmodulin-dependent regulation of a lipid binding domain in the v-SNARE synaptobrevin and its role in vesicular fusion. *Biol Cell*. 95:459-64.

30. Dulubova, I., S. Sugita, S. Hill, M. Hosaka, I. Fernandez, T.C. Sudhof, and J. Rizo. 1999. A conformational switch in syntaxin during exocytosis: role of munc18. *Embo J*. 18:4372-82.

31. Fasshauer, D. 2003. Structural insights into the SNARE mechanism. *Biochim Biophys Acta*. 1641:87-97.

32. Fasshauer, D., and M. Margittai. 2004. A transient N-terminal interaction of SNAP-25 and syntaxin nucleates SNARE assembly. *J Biol Chem*. 279:7613-21.

33. Fasshauer, D., H. Otto, W.K. Eliason, R. Jahn, and A.T. Brunger. 1997. Structural changes are associated with soluble N-ethylmaleimide-sensitive fusion protein attachment protein receptor complex formation. *J Biol Chem*. 272:28036-41.

34. Fassio, A., R. Sala, G. Bonanno, M. Marchi, and M. Raiteri. 1999. Evidence for calcium-dependent vesicular transmitter release insensitive to tetanus toxin and botulinum toxin type F. *Neuroscience*. 90:893-902.

35. Fernandez-Chacon, R., A. Konigstorfer, S.H. Gerber, J. Garcia, M.F. Matos, C.F. Stevens, N. Brose, J. Rizo, C. Rosenmund, and T.C. Sudhof. 2001. Synaptotagmin I functions as a calcium regulator of release probability. *Nature*. 410:41-9.

36. Garcia E.P., E. Gatti, M. Butler, J. Burton, and P. De Camilli. 1994. A rat brain Sec1 homologue related to Rop and UNC18 interacts with syntaxin. *Proc Natl Acad Sci U S A*. 91:2003-7.

37. Geppert, M., B.T. Archer, 3rd, and T.C. Sudhof. 1991. Synaptotagmin II. A novel differentially distributed form of synaptotagmin. *J Biol Chem*. 266:13548-52.

38. Geppert, M., Y. Goda, C.F. Stevens, and T.C. Sudhof. 1997. The small GTP-binding protein Rab3A regulates a late step in synaptic vesicle fusion. *Nature*. 387:810-4.

39. Gerona, R.R., E.C. Larsen, J.A. Kowalchyk, and T.F. Martin. 2000. The C terminus of SNAP25 is essential for Ca(2+)-dependent binding of synaptotagmin to SNARE complexes. *J Biol Chem*. 275:6328-36.

40. Gundelfinger, E.D., M.M. Kessels, and B. Qualmann. 2003. Temporal and spatial coordination of exocytosis and endocytosis. *Nat Rev Mol Cell Biol*. 4:127-39.

41. Hanson, P.I., H. Otto, N. Barton, and R. Jahn. 1995. The N-ethylmaleimide-sensitive fusion protein and alpha-SNAP induce a conformational change in syntaxin. *J Biol Chem*. 270:16955-61.

42. Hanson, P.I., R. Roth, H. Morisaki, R. Jahn, and J.E. Heuser. 1997. Structure and conformational changes in NSF and its membrane receptor complexes visualized by quick-freeze/deep-etch electron microscopy. *Cell*. 90:523-35.

43. Hata, Y., C.A. Slaughter, and T.C. Sudhof. 1993. Synaptic vesicle fusion complex contains unc-18 homologue bound to syntaxin. *Nature*. 366:347-51.

44. Hay, J.C., and T.F. Martin. 1992. Resolution of regulated secretion into sequential MgATP-dependent and calcium-dependent stages mediated by distinct cytosolic proteins. *J Cell Biol*. 119:139-51.

45. Hay, J.C., and T.F. Martin. 1993. Phosphatidylinositol transfer protein required for ATP-dependent priming of Ca(2+)-activated secretion. *Nature*. 366:572-5.

46. Hayashi, T., H. McMahon, S. Yamasaki, T. Binz, Y. Hata, T.C. Sudhof, and H. Niemann. 1994. Synaptic vesicle membrane fusion complex: action of clostridial neurotoxins on assembly. *Embo J*. 13:5051-61.

47. Hayashi, T., S. Yamasaki, S. Nauenburg, T. Binz, and H. Niemann. 1995. Disassembly of the reconstituted synaptic vesicle membrane fusion complex in vitro. *Embo J*. 14:2317-25.

48. Heidelberger, R. 1998. Adenosine triphosphate and the late steps in calcium-dependent exocytosis at a ribbon synapse. *J Gen Physiol*. 111:225-41.

49. Heinemann, C., R.H. Chow, E. Neher, and R.S. Zucker. 1994. Kinetics of the secretory response in bovine chromaffin cells following flash photolysis of caged Ca2+. *Biophys J*. 67:2546-57.

50. Heumann, R., V. Kachel, and H. Thoenen. 1983. Relationship between NGF-mediated volume increase and "priming effect" in fast and slow reacting clones of PC12 pheochromocytoma cells. Role of cAMP. *Exp Cell Res*. 145:179-90.

51. Holroyd, P., T. Lang, D. Wenzel, P. De Camilli, and R. Jahn. 2002. Imaging direct, dynamin-dependent recapture of fusing secretory granules on plasma membrane lawns from PC12 cells. *Proc Natl Acad Sci U S A*. 99:16806-11.

52. Holz, R.W., M.A. Bittner, S.C. Peppers, R.A. Senter, and D.A. Eberhard. 1989. MgATP-independent and MgATP-dependent exocytosis. Evidence that MgATP primes adrenal chromaffin cells to undergo exocytosis. *J Biol Chem*. 264:5412-9.

53. Hua, S.Y., and M.P. Charlton. 1999. Activity-dependent changes in partial VAMP complexes during neurotransmitter release. *Nat Neurosci*. 2:1078-83.

54. Hua, Y., and R.H. Scheller. 2001. Three SNARE complexes cooperate to mediate membrane fusion. *Proc Natl Acad Sci U S A*. 98:8065-70.

55. Ishizuka, T., H. Saisu, S. Odani, and T. Abe. 1995. Synaphin: a protein associated with the docking/fusion complex in presynaptic terminals. *Biochem Biophys Res Commun*. 213:1107-14.

56. Jahn, R., and H. Grubmuller. 2002. Membrane fusion. *Curr Opin Cell Biol*. 14:488-95.

57. Jahn, R., and P.I. Hanson. 1998. Membrane fusion. SNAREs line up in new environment. *Nature*. 393:14-5.

58. Jahn, R., T. Lang, and T.C. Sudhof. 2003. Membrane fusion. *Cell*. 112:519-33.

59. Kibble, A.V., R.J. Barnard, and R.D. Burgoyne. 1996. Patch-clamp capacitance analysis of the effects of alpha-SNAP on exocytosis in adrenal chromaffin cells. *J Cell Sci*. 109 (Pt 9):2417-22.

60. Koga, T., and M. Takahashi. 2004. Quantal size of catecholamine release from rat chromaffin cells is regulated by tonic activity of protein kinase A. *Neurosci Lett*. 360:145-8.

61. Kumakura, K., K. Sasaki, T. Sakurai, M. Ohara-Imaizumi, H. Misonou, S. Nakamura, Y. Matsuda, and Y. Nonomura. 1994. Essential role of myosin light chain kinase in the mechanism for MgATP-dependent priming of exocytosis in adrenal chromaffin cells. *J Neurosci*. 14:7695-703.

62. Lang, T., D. Bruns, D. Wenzel, D. Riedel, P. Holroyd, C. Thiele, and R. Jahn. 2001. SNAREs are concentrated in cholesterol-dependent clusters that define docking and fusion sites for exocytosis. *Embo J*. 20:2202-13.

63. Lang, T., M. Margittai, H. Holzler, and R. Jahn. 2002. SNAREs in native plasma membranes are active and readily form core complexes with endogenous and exogenous SNAREs. *J Cell Biol*. 158:751-60.

64. Lawrence, G.W., U. Weller, and J.O. Dolly. 1994. Botulinum A and the light chain of tetanus toxins inhibit distinct stages of Mg.ATP-dependent catecholamine exocytosis from permeabilised chromaffin cells. *Eur J Biochem*. 222:325-33.

65. Lin, R.C., and R.H. Scheller. 1997. Structural organization of the synaptic exocytosis core complex. *Neuron*. 19:1087-94.

66. Linial, M., and D. Parnas. 1996. Deciphering neuronal secretion: tools of the trade. *Biochim Biophys Acta*. 1286:117-52.

67. Link, E., L. Edelmann, J.H. Chou, T. Binz, S. Yamasaki, U. Eisel, M. Baumert, T.C. Sudhof, H. Niemann, and R. Jahn. 1992. Tetanus toxin action: inhibition of neurotransmitter release linked to synaptobrevin proteolysis. *Biochem Biophys Res Commun*. 189:1017-23.

68. Littleton, J.T., E.R. Chapman, R. Kreber, M.B. Garment, S.D. Carlson, and B. Ganetzky. 1998. Temperature-sensitive paralytic mutations demonstrate that synaptic exocytosis requires SNARE complex assembly and disassembly. *Neuron*. 21:401-13.

69. McMahon, H.T., M. Missler, C. Li, and T.C. Sudhof. 1995. Complexins: cytosolic proteins that regulate SNAP receptor function. *Cell*. 83:111-9.

70. McMahon, H.T., and T.C. Sudhof. 1995. Synaptic core complex of synaptobrevin, syntaxin, and SNAP25 forms high affinity alpha-SNAP binding site. *J Biol Chem*. 270:2213-7.

71. Martin, T.F. 1989. Cell cracking: permeabilizing cells to macromolecular probes. *Methods Enzymol*. 168:225-33.

72. Martin, T.F., J.C. Hay, A. Banerjee, V.A. Barry, K. Ann, H.C. Yom, B.W. Porter, and J.A. Kowalchyk. 1995. Late ATP-dependent and Ca++-activated steps of dense core granule exocytosis. *Cold Spring Harb Symp Quant Biol*. 60:197-204.

73. Martin, T.F., and J.A. Kowalchyk. 1997. Docked secretory vesicles undergo Ca2+-activated exocytosis in a cell-free system. *J Biol Chem*. 272:14447-53.

74. Martin, T.F. 2003. Tuning exocytosis for speed: fast and slow modes. *Biochim Biophys Acta*. 1641:157-65.

75. Montecucco, C., G. Schiavo, Z. Gao, E. Bauerlein, P. Boquet, and B.R. DasGupta. 1988. Interaction of botulinum and tetanus toxins with the lipid bilayer surface. *Biochem J*. 251:379-83.

76. Nagy, G., U. Matti, R.B. Nehring, T. Binz, J. Rettig, E. Neher, and J.B. Sorensen. 2002. Protein kinase C-dependent phosphorylation of synaptosome-associated protein of 25 kDa at Ser187 potentiates vesicle recruitment. *J Neurosci*. 22:9278-86.

77. Niemann, H., J. Blasi, and R. Jahn. 1994. Clostridial neurotoxins: new tools for dissecting exocytosis. *Trends Cell Biol*. 4:179-85.

78. Novick, P., and M. Zerial. 1997. The diversity of Rab proteins in vesicle transport. *Curr Opin Cell Biol*. 9:496-504.

79. Olivo-Marin J.C. 2002. Extraction of spots in biological images using multiscale products. *Pattern Recognition* 35:1989–1996.

80. Otto, H., P.I. Hanson, E.R. Chapman, J. Blasi, and R. Jahn. 1995. Poisoning by botulinum neurotoxin A does not inhibit formation or disassembly of the synaptosomal fusion complex. *Biochem Biophys Res Commun*. 212:945-52.

81. Oyler, G.A., G.A. Higgins, R.A. Hart, E. Battenberg, M. Billingsley, F.E. Bloom, and M.C. Wilson. 1989. The identification of a novel synaptosomal-associated protein, SNAP-25, differentially expressed by neuronal subpopulations. *J Cell Biol*. 109:3039-52.

82. Patel, S., and M. Latterich. 1998. The AAA team: related ATPases with diverse functions. *Trends Cell Biol*. 8:65-71.

83. Perin, M.S., V.A. Fried, G.A. Mignery, R. Jahn, and T.C. Sudhof. 1990. Phospholipid binding by a synaptic vesicle protein homologous to the regulatory region of protein kinase C. *Nature*. 345:260-3.

84. Parsons, T.D., J.R. Coorssen, H. Horstmann, and W. Almers. 1995. Docked granules, the exocytic burst, and the need for ATP hydrolysis in endocrine cells. *Neuron*. 15:1085-96.

85. Patterson, G.H., S.M. Knobel, W.D. Sharif, S.R. Kain, and D.W. Piston. 1997. Use of the green fluorescent protein and its mutants in quantitative fluorescence microscopy. *Biophys J*. 73:2782-90.

86. Pevsner, J., S.C. Hsu, and R.H. Scheller. 1994. n-Sec1: a neural-specific syntaxin-binding protein. *Proc Natl Acad Sci U S A*. 91:1445-9.

87. Pfeffer, S.R. 1999. Transport-vesicle targeting: tethers before SNAREs. *Nat Cell Biol*. 1:E17-22.

88. Rettig, J., and E. Neher. 2002. Emerging roles of presynaptic proteins in Ca++-triggered exocytosis. *Science*. 298:781-5.

89. Rohrbough, J., and K. Broadie. 2005. Lipid regulation of the synaptic vesicle cycle. *Nat Rev Neurosci*. 6:139-50.

90. Ryan, T.A. 1998. Probing a complex question: when are SNARE proteins ensnared? *Nat Neurosci*. 1:175-6.

91. Schiavo, G., M. Matteoli, and C. Montecucco. 2000. Neurotoxins affecting neuroexocytosis. *Physiol Rev*. 80:717-66.

92. Schuette, C.G., K. Hatsuzawa, M. Margittai, A. Stein, D. Riedel, P. Kuster, M. Konig, C. Seidel, and R. Jahn. 2004. Determinants of liposome fusion mediated by synaptic SNARE proteins. *Proc Natl Acad Sci U S A*. 101:2858-63.

93. Sogaard, M., K. Tani, R.R. Ye, S. Geromanos, P. Tempst, T. Kirchhausen, J.E. Rothman, and T. Sollner. 1994. A rab protein is required for the assembly of SNARE complexes in the docking of transport vesicles. *Cell*. 78:937-48.

94. Sollner, T., S.W. Whiteheart, M. Brunner, H. Erdjument-Bromage, S. Geromanos, P. Tempst, and J.E. Rothman. 1993. SNAP receptors implicated in vesicle targeting and fusion. *Nature*. 362:318-24.

95. Sollner, T.H. 2003. Regulated exocytosis and SNARE function (Review). *Mol Membr Biol*. 20:209-20.

96. Sorensen, J.B. 2004. Formation, stabilisation and fusion of the readily releasable pool of secretory vesicles. *Pflugers Arch*. 448:347-62.

97. Steyer, J.A., H. Horstmann, and W. Almers. 1997. Transport, docking and exocytosis of single secretory granules in live chromaffin cells. *Nature*. 388:474-8.

98. Sutton, R.B., D. Fasshauer, R. Jahn, and A.T. Brunger. 1998. Crystal structure of a SNARE complex involved in synaptic exocytosis at 2.4 A resolution. *Nature*. 395:347-53.

99. Thureson-Klein, A. 1983. Exocytosis from large and small dense cored vesicles in noradrenergic nerve terminals. *Neuroscience*. 10:245-59.

100. Toonen, R.F., and M. Verhage. 2003. Vesicle trafficking: pleasure and pain from SM genes. *Trends Cell Biol*. 13:177-86.

101. Tooze, S.A., G.J. Martens, and W.B. Huttner. 2001. Secretory granule biogenesis: rafting to the SNARE. *Trends Cell Biol*. 11:116-22.

102. Trimble, W.S., D.M. Cowan, and R.H. Scheller. 1988. VAMP-1: a synaptic vesicle-associated integral membrane protein. *Proc Natl Acad Sci U S A*. 85:4538-42.

103. van den Hoff, M.J., A.F. Moorman, and W.H. Lamers. 1992. Electroporation in 'intracellular' buffer increases cell survival. *Nucleic Acids Res*. 20:2902.

104. Voets, T., R.F. Toonen, E.C. Brian, H. de Wit, T. Moser, J. Rettig, T.C. Sudhof, E. Neher, and M. Verhage. 2001. Munc18-1 promotes large dense-core vesicle docking. *Neuron*. 31:581-91.

105. Vu, N.D., and P.D. Wagner. 1993. Stimulation of secretion in permeabilized PC12 cells by adenosine 5'-[gamma-thio]triphosphate: possible involvement of nucleoside diphosphate kinase. *Biochem J*. 296 (Pt 1):169-74.

106. Wang, L., C. Ungermann, and W. Wickner. 2000. The docking of primed vacuoles can be reversibly arrested by excess Sec17p (alpha-SNAP). *J Biol Chem*. 275:22862-7.

107. Weber, T., B.V. Zemelman, J.A. McNew, B. Westermann, M. Gmachl, F. Parlati, T.H. Sollner, and J.E. Rothman. 1998. SNAREpins: minimal machinery for membrane fusion. *Cell*. 92:759-72.

108. Wenk, M.R., and P. De Camilli. 2004. Protein-lipid interactions and phosphoinositide metabolism in membrane traffic: insights from vesicle recycling in nerve terminals. *Proc Natl Acad Sci U S A*. 101:8262-9.

109. Whalley, T., I. Crossley, and M. Whitaker. 1991. Phosphoprotein inhibition of calcium-stimulated exocytosis in sea urchin eggs. *J Cell Biol*. 113:769-78.

110. Whiteheart, S.W., T. Schraw, and E.A. Matveeva. 2001. N-ethylmaleimide sensitive factor (NSF) structure and function. *Int Rev Cytol*. 207:71-112.

111. Xu, T., U. Ashery, R.D. Burgoyne, and E. Neher. 1999a. Early requirement for alpha-SNAP and NSF in the secretory cascade in chromaffin cells. *Embo J*. 18:3293-304.

112. Xu, T., T. Binz, H. Niemann, and E. Neher. 1998. Multiple kinetic components of exocytosis distinguished by neurotoxin sensitivity. *Nat Neurosci*. 1:192-200.

113. Xu, T., B. Rammner, M. Margittai, A.R. Artalejo, E. Neher, and R. Jahn. 1999b. Inhibition of SNARE complex assembly differentially affects kinetic components of exocytosis. *Cell*. 99:713-22.

114. Yamasaki, S., A. Baumeister, T. Binz, J. Blasi, E. Link, F. Cornille, B. Roques, E.M. Fykse, T.C. Sudhof, R. Jahn, and et al. 1994. Cleavage of members of the synaptobrevin/VAMP family by types D and F botulinal neurotoxins and tetanus toxin. *J Biol Chem*. 269:12764-72.

115. Zerial, M., and H. McBride. 2001. Rab proteins as membrane organizers. *Nat Rev Mol Cell Biol*. 2:107-17.

116. Ziv, N.E., and C.C. Garner. 2004. Cellular and molecular mechanisms of presynaptic assembly. *Nat Rev Neurosci*. 5:385-99.

Curriculum Vitae

Personal Details:

Name:	Marcin Mirosław Barszczewski
Nationality:	Polish
Date of Birth:	26.01.1977
Place of Birth:	Warsaw, Poland
Contact Details (Private):	Valentinsbreite 15 37077 Göttingen Germany Tel: 0551-3067226
Contact Details (Work):	Max-Planck-Institute for Biophysical Chemistry Division of Neurobiology Am Fassberg 11 37077 Göttingen Germany Tel: 0551-201-1670 Fax: 0551-201-1499 E-mail: mbarszc@gwdg.de

Education:

School Education:

1984 – 86	Primary School Nr 175, Warsaw
1986 – 87	Primary School (Polish Embassy), Al-Marj, Libya
1987 – 92	Primary School Nr 175, Warsaw
1992 - 96	VIth High School “T.Reytan”, Warsaw

University Education:

Oct 1996 – Sept 2001:	Studies of Biology and Biotechnology, Warsaw University
Sep 2000 – May 2005:	International M.Sc./PhD Programme in Neurosciences 2000 University of Göttingen, Germany

Aug 2001	M.Sc. Diploma with Honors in Biology/Biotechnology
Oct 2001 – May 2005:	PhD Student, MPI for Biophysical Chemistry, Department of Neurobiology Göttingen, Germany

Acknowledgements

I thank Prof. Reinhard Jahn for giving me the opportunity to work in his department in stimulating conditions and advanced circumstances. I am grateful to Dr Thorsten Lang for his supervision and patience and help throughout the course of my studies. I owe many thanks to Dr Rainer Heintzmann who was instrumental during the development of the Cantata workspaces and to Dr Gottfried Mieskes who helped me on every day basis with numerous little issues in the laboratory.

I am also indebted to Prof. Erwin Neher and Prof. Nils Brose for their support as my thesis committee and for their assistance whenever it was needed.

My work also was supported by numerous members of the Neurobiology Department to whom I deeply grateful for the friendly working atmosphere and their presence during many difficult moments. Especially big “thanks” go to Sophie, Anand, Alexander, Matthew, Phil and Stephan for many good moments spent and enjoyed together.

I would also like to thank Dr. Simone Cardoso de Oliviera, Sandra Drube, Dr. Steffen Burkhard, Dr. Dorotee Wegener and Prof. Michael Hörner for all of their support in administrative matters and for creating a fantastic environment for the graduate students of Göttingen.

Finally, I would like to express my deepest gratitude to my Parents, Krysia and Martin for their constant support during all tough times.

Dziękuję Wam za Waszą wiarę i miłość.